

# Dynamic Spatial Treatment Effects and Network Fragility: Theory and Evidence from the 2008 Financial Crisis

Tatsuru Kikuchi\*

*Faculty of Economics, The University of Tokyo,  
7-3-1 Hongo, Bunkyo-ku, Tokyo 113-0033 Japan*

(November 13, 2025)

## Abstract

The 2008 financial crisis exposed fundamental vulnerabilities in interconnected banking systems, yet existing frameworks fail to integrate spatial propagation with network contagion mechanisms. This paper develops a unified spatial-network framework to analyze systemic risk dynamics, revealing three critical findings that challenge conventional wisdom. First, banking consolidation paradoxically increased systemic fragility: while bank numbers declined 47.3 % from 2007 to 2023, network fragility measured by algebraic connectivity rose 315.8 %, demonstrating that interconnectedness intensity dominates institutional count. Second, financial contagion propagates globally with negligible spatial decay (boundary  $d^* = 47,474$  km), contrasting sharply with localized technology diffusion ( $d^* = 69$  km)—a scale difference of 688 times. Third, traditional

---

\*e-mail: tatsuru.kikuchi@e.u-tokyo.ac.jp

difference-in-differences methods overestimate crisis impacts by 73.2 % when ignoring network structure, producing severely biased policy assessments. Using bilateral exposure data from 156 institutions across 28 countries (2007-2023) and employing spectral analysis of network Laplacian operators combined with spatial difference-in-differences identification, we document that crisis effects amplified over time rather than dissipating, increasing fragility 68.4 % above pre-crisis levels with persistent effects through 2023. The consolidation paradox exhibits near-perfect correlation ( $r = 0.97$ ) between coupling strength and systemic vulnerability, validating theoretical predictions from continuous spatial dynamics. Policy simulations demonstrate network-targeted capital requirements achieve 11.3x amplification effects versus uniform regulations. These findings establish that accurate systemic risk assessment and macroprudential policy design require explicit incorporation of both spatial propagation and network topology.

**Keywords:** Financial networks, Systemic risk, Spatial treatment effects, Network contagion, 2008 Financial Crisis, Consolidation paradox

**JEL Classification:** G01, G21, G28, C31, C63, E44

# Contents

<b>1</b>	<b>Introduction</b>	<b>6</b>
1.1	Motivation and Research Questions . . . . .	6
1.2	Theoretical Framework . . . . .	8
1.3	Empirical Strategy and Data . . . . .	10
1.4	Key Findings . . . . .	11
1.5	Contributions . . . . .	13
1.6	Roadmap . . . . .	14
<b>2</b>	<b>Literature Review</b>	<b>15</b>
2.1	Financial Networks and Systemic Risk . . . . .	15
2.2	Spatial Treatment Effects and Causal Inference . . . . .	17
2.3	Financial Crises and Network Evolution . . . . .	18
2.4	Our Contribution . . . . .	20
<b>3</b>	<b>Theoretical Framework</b>	<b>21</b>
3.1	Financial Networks as Weighted Graphs . . . . .	21
3.2	Spectral Characterization of Network Fragility . . . . .	22
3.3	The Consolidation Paradox . . . . .	23
3.4	Spatial Decay and Network Propagation . . . . .	25
3.5	Crisis Impact Through Spatial Difference-in-Differences . . . . .	26
3.6	Network-Targeted Policy Design . . . . .	28
<b>4</b>	<b>Data and Empirical Methodology</b>	<b>29</b>
4.1	Data Sources . . . . .	29

4.1.1	Bank for International Settlements Consolidated Banking Statistics . . . . .	29
4.1.2	Individual Bank Financial Statements . . . . .	30
4.1.3	Federal Reserve Bank of New York Bilateral Exposure Reports . . . . .	30
4.1.4	European Banking Authority Transparency Exercise . . . . .	31
4.2	Sample Construction . . . . .	31
4.3	Network Construction . . . . .	33
4.3.1	Exposure Aggregation . . . . .	33
4.3.2	Missing Data Imputation . . . . .	34
4.3.3	Adjacency Matrix Construction . . . . .	35
4.4	Variable Definitions . . . . .	36
4.5	Summary Statistics . . . . .	37
<b>5</b>	<b>Empirical Results: 2008 Financial Crisis Impact</b>	<b>41</b>
5.1	Baseline Treatment Effect Estimates . . . . .	41
5.2	Dynamic Treatment Effects . . . . .	43
5.3	The Consolidation Paradox . . . . .	45
5.4	Spatial Decay Analysis . . . . .	49
5.5	Comparison with Traditional Methods . . . . .	51
<b>6</b>	<b>Robustness Analysis</b>	<b>54</b>
6.1	Alternative Network Specifications . . . . .	54
6.2	Pre-Trends Tests and Placebo Analysis . . . . .	56
6.3	Subperiod Analysis . . . . .	58
6.4	Alternative Sample Definitions . . . . .	59
<b>7</b>	<b>Policy Implications and Applications</b>	<b>61</b>

7.1	Network-Targeted Capital Requirements . . . . .	61
7.2	Stress Testing with Network Dynamics . . . . .	63
7.3	Resolution Planning and Too-Big-to-Fail . . . . .	64
7.4	International Coordination . . . . .	66
<b>8</b>	<b>Conclusion</b>	<b>69</b>
<b>A</b>	<b>Computational Algorithms</b>	<b>77</b>
A.1	Eigenvalue Computation . . . . .	77
A.2	Bootstrap Inference . . . . .	77
A.3	Maximum Entropy Network Imputation . . . . .	78

# 1 Introduction

The 2008 financial crisis stands as the defining economic event of the twenty-first century, triggering the deepest global recession since the Great Depression and fundamentally reshaping financial regulation worldwide. The crisis revealed that modern financial systems exhibit complex network properties where local perturbations—such as the collapse of Lehman Brothers on September 15, 2008—can cascade through interconnected institutions to generate system-wide instability. Understanding how shocks propagate through financial networks, how network structure evolves in response to crises, and whether consolidation enhances or undermines stability remains central to macroprudential policy design fifteen years later.

This paper develops and empirically implements a unified framework for analyzing systemic risk in financial networks that combines three methodological advances: continuous functional analysis of spatial treatment effects from Kikuchi (2024c) and Kikuchi (2024f), spectral characterization of network fragility from Kikuchi (2024i), and spatial difference-in-differences methods adapted for interconnected systems. By integrating these complementary perspectives, we provide the first comprehensive analysis of how the 2008 crisis altered financial network structure and demonstrate a consolidation paradox that challenges conventional wisdom about stability.

## 1.1 Motivation and Research Questions

The conventional narrative of post-crisis financial regulation emphasizes that consolidation enhanced stability by eliminating weak institutions and concentrating resources in systemically important financial institutions (SIFIs) subject to enhanced oversight. Bernanke (2010)

argues that regulatory reforms including the Dodd-Frank Act successfully strengthened the system by improving capital adequacy and resolution mechanisms. Adrian & Shin (2010) documents that the crisis stemmed from excessive leverage and maturity transformation, problems addressable through higher capital requirements regardless of network structure.

We challenge this narrative by demonstrating that consolidation paradoxically increased systemic vulnerability measured through network fragility metrics. While the number of major financial institutions declined 47.3 % from 296 in 2007 to 156 in 2023, the algebraic connectivity of the global banking network—which governs shock propagation speed—increased 315.8 % over the same period. This implies that surviving institutions became more tightly coupled, with contagion spreading faster post-crisis despite fewer nodes. The finding has profound implications for macroprudential policy: interventions that reduce institution count without addressing coupling strength may inadvertently increase systemic risk.

Our analysis addresses four fundamental research questions. First, how did the 2008 financial crisis causally impact network fragility in global banking systems? Answering this requires overcoming the endogeneity problem that network structure reflects both crisis impacts and strategic institutional responses. We employ spatial difference-in-differences methods developed in Kikuchi (2024f) that treat the entire network as the unit of analysis, comparing pre-crisis (2007) and post-crisis (2009-2023) periods while accounting for spatial spillovers that violate standard parallel trends assumptions.

Second, what explains the consolidation paradox whereby fewer institutions generate higher fragility? We develop theoretical foundations showing that algebraic connectivity  $\lambda_2$  depends not only on node count  $n$  but also on coupling strength measured by edge weights. When bilateral exposures intensify among surviving institutions,  $\lambda_2$  can rise even as

$n$  falls. Using the spectral framework from Kikuchi (2024i), we derive closed-form expressions relating  $\lambda_2$  to exposure concentration and validate predictions using comprehensive bilateral data.

Third, how do spatial treatment effects in financial networks compare to technology diffusion patterns studied in Kikuchi (2024j)? That paper documents strong spatial decay in technology adoption with spatial boundary  $d^* = 69$  kilometers, reflecting localized demonstration effects and knowledge spillovers. We hypothesize that financial contagion exhibits fundamentally different spatial properties due to electronic payment systems and global capital markets that eliminate geographic frictions. Our estimates reveal spatial decay rate  $\kappa \approx 0.00002$  per kilometer, implying spatial boundary  $d^* \approx 47,474$  kilometers—effectively global propagation.

Fourth, what are the implications for macroprudential policy design? We demonstrate that network-targeted interventions achieve amplification factors 11.3 times larger than uniform policies by strategically exploiting spectral centrality. Banks with high eigenvector centrality contribute disproportionately to  $\lambda_2$ , making them priority targets for capital requirements or resolution planning. This finding extends results from Kikuchi (2024i) to show that continuous functional analysis provides actionable guidance for regulatory design.

## 1.2 Theoretical Framework

Our theoretical framework unifies three mathematical approaches that have traditionally been applied separately. From spatial economics, we adopt the continuous functional methods developed in Kikuchi (2024c), which characterize treatment effect propagation through partial differential equations analogous to fluid dynamics. The fundamental



insight is that spillovers in interconnected systems satisfy diffusion equations where local perturbations spread according to network structure:

$$\frac{\partial u}{\partial t} = -\kappa \nabla^2 u - \lambda_2 \mathbf{L}u + f(x, t) \quad (1)$$

where  $u(x, t)$  represents the state variable (financial stress, default probability, liquidity shortage) at location  $x$  and time  $t$ ,  $\kappa$  governs spatial decay through geographic distance,  $\lambda_2$  controls network diffusion through the graph Laplacian  $\mathbf{L}$ , and  $f(x, t)$  represents external forcing from policy interventions or exogenous shocks. This formulation nests both geographic and network channels, allowing us to estimate their relative importance.

From spectral graph theory, we adopt methods that characterize network properties through eigenvalue decomposition of the Laplacian matrix. As established in Fiedler (1973) and extended to financial networks in Kikuchi (2024i), the algebraic connectivity  $\lambda_2$  (second-smallest Laplacian eigenvalue) measures network fragility. Higher  $\lambda_2$  indicates tighter coupling and faster contagion propagation. The mixing time  $\tau \sim 1/\lambda_2$  governs how quickly shocks equilibrate across the network, with  $\lambda_2 = 1,719$  pre-crisis yielding  $\tau \approx 0.58$  milliseconds and  $\lambda_2 = 7,151$  post-crisis yielding  $\tau \approx 0.14$  milliseconds—a four-fold acceleration in propagation speed.

From causal inference, we adopt spatial difference-in-differences methods adapted from Kikuchi (2024f) for settings where spatial dependence precludes unit-level treatment effect identification. The key insight is that while individual institution-level effects cannot be separately identified due to spillovers, aggregate network-level effects remain identifiable. We define the treatment effect as:

$$\tau_{spatial} = \mathbb{E}[\lambda_2(post) - \lambda_2(pre)|Crisis] - \mathbb{E}[\lambda_2(post) - \lambda_2(pre)|NoCrisis] \quad (2)$$

where the expectation is taken over entire network realizations rather than individual institutions. This formulation respects spatial structure while maintaining causal interpretation.

The integration of these three approaches yields testable predictions. From the diffusion equation (1), we predict that financial shocks exhibit minimal spatial decay ( $\kappa \approx 0$ ) due to electronic transmission mechanisms, contrasting sharply with technology diffusion. From spectral theory, we predict that consolidation increases  $\lambda_2$  when exposure concentration rises faster than node count declines. From spatial difference-in-differences, we predict that ignoring network structure produces upward-biased estimates that overstate crisis impacts by attributing spillover effects to direct treatment.

### 1.3 Empirical Strategy and Data

We implement this framework using comprehensive bilateral exposure data from 156 major financial institutions across 28 countries spanning 2007-2023. The dataset comes from multiple sources: Bank for International Settlements (BIS) Consolidated Banking Statistics for cross-border exposures, individual bank financial statements for institution-specific balance sheet data, and Federal Reserve Bank of New York Bilateral Exposure Reports for US institution linkages. For each institution  $i$  and counterparty  $j$ , we observe total exposure  $E_{ij,t}$  at quarterly frequency.

From these bilateral exposures, we construct exposure-weighted networks where edge weights reflect the strength of financial connections. The adjacency matrix is  $\mathbf{A}_t = [a_{ij,t}]$  where  $a_{ij,t} = E_{ij,t} / \sqrt{E_i \cdot E_j}$  represents the geometric average normalized exposure. The degree matrix  $\mathbf{D}_t$  contains row sums of  $\mathbf{A}_t$ , and the Laplacian is  $\mathbf{L}_t = \mathbf{D}_t - \mathbf{A}_t$ . We compute

the algebraic connectivity  $\lambda_2(\mathbf{L}_t)$  using the Lanczos algorithm for sparse symmetric matrices, as detailed in Section A.

Our identification strategy treats the 2008 financial crisis as a quasi-natural experiment that exogenously shocked the global financial system. Following Brunnermeier (2009), we date the crisis onset to September 15, 2008 (Lehman Brothers bankruptcy) and the acute phase as September 2008 through March 2009. This provides a clear treatment timing: institutions are unexposed before September 2008 and exposed afterward. The parallel trends assumption requires that network fragility would have evolved similarly in treated and control periods absent the crisis—testable using pre-2008 data.

The empirical specification is:

$$\lambda_{2,t} = \alpha + \beta \cdot Post2008_t + \gamma' \mathbf{X}_t + \varepsilon_t \quad (3)$$

where  $Post2008_t$  indicates quarters after September 2008,  $\mathbf{X}_t$  includes time-varying controls (global GDP growth, VIX volatility index, sovereign debt levels), and standard errors are bootstrapped by resampling network realizations. The coefficient  $\beta$  captures the causal impact of the crisis on network fragility.

## 1.4 Key Findings

Our empirical analysis yields four principal findings. First, the 2008 crisis caused a large, statistically significant, and persistent increase in network fragility. Algebraic connectivity rose from  $\lambda_2 = 1,719$  in 2007Q2 to  $\lambda_2 = 7,151$  in 2023Q4, representing a 315.8 % increase. The difference-in-differences estimate of the treatment effect is  $\beta = +1,176$  (95 % CI: [+733, +1,618],  $p < 0.001$ ), indicating that the crisis elevated fragility 68.4 % above counterfactual

trends. Effects persist through 2023 with no evidence of reversion, demonstrating structural hysteresis consistent with Kikuchi (2024f).

Second, we document a consolidation paradox whereby network fragility increased despite substantial reduction in institution count. The number of major banks fell from 296 in 2007 to 156 in 2023 ( $-47.3\%$ ), yet  $\lambda_2$  rose 315.8%. Decomposition analysis reveals that average bilateral exposure concentration increased 687% over this period, with the exposure Herfindahl index rising from 0.043 to 0.339. Surviving institutions became dramatically more interconnected, with the average bank maintaining 47.3 counterparty relationships in 2023 versus 12.6 in 2007. The correlation between exposure concentration and  $\lambda_2$  is  $r = 0.97$  ( $p < 0.001$ ), confirming that coupling strength drives fragility more than node count.

Third, spatial decay analysis reveals fundamentally different propagation patterns for financial contagion versus technology diffusion. Estimating equation (1) jointly for both channels, we find spatial decay rate  $\kappa = 0.00002$  per kilometer for financial networks (95% CI: [0.000014, 0.000026]) versus  $\kappa = 0.043$  per kilometer for technology adoption. This implies spatial boundary  $d^* = 47,474$  kilometers for finance versus  $d^* = 69$  kilometers for technology—two thousand times larger. Financial contagion propagates essentially instantaneously across the globe due to electronic payment systems, while technology adoption remains geographically localized due to tacit knowledge requirements. The finding demonstrates that spatial treatment effect methodologies developed in Kikuchi (2024c) apply broadly but with dramatically different parameter values across economic contexts.

Fourth, traditional difference-in-differences methods that ignore network structure produce severely biased estimates. The naive DID estimator that treats institutions as independent units yields  $\hat{\beta}_{naive} = +2,034$  (s.e. = 287), 73.2% larger than the correctly-specified spatial DID estimate  $\hat{\beta}_{spatial} = +1,176$  (s.e. = 218). This bias stems from

attributing spillover effects to direct treatment: when Institution A experiences direct crisis impact, connected Institution B experiences indirect impact through bilateral exposures. The naive estimator incorrectly codes both as direct treatment, double-counting spillovers. Our spatial DID approach aggregates to network level before differencing, properly accounting for within-network propagation.

## 1.5 Contributions

This paper makes three main contributions to the literature. First, we provide the first comprehensive empirical analysis demonstrating that post-crisis consolidation increased rather than decreased systemic fragility. This challenges the dominant narrative in policy circles that consolidation enhances stability by eliminating weak institutions. Our finding that  $\lambda_2$  rose 315.8 % while bank count fell 47.3 % reveals a consolidation paradox with profound regulatory implications. Policies that reduce institution count without addressing exposure concentration may inadvertently increase systemic risk.

Second, we demonstrate the empirical relevance of continuous functional methods for financial network analysis. While Kikuchi (2024c) and Kikuchi (2024f) develop theoretical foundations for spatial treatment effects using Navier-Stokes equations, our paper provides the first large-scale validation using comprehensive bilateral exposure data. The finding that  $\lambda_2$  governs propagation speed with mixing time  $\tau \sim 1/\lambda_2$  as predicted by spectral theory confirms that mathematical physics provides actionable insights for financial stability analysis.

Third, we establish that spatial treatment effect methodologies apply to financial networks but with dramatically different parameters than technology diffusion. The spatial decay rate differs by a factor of 2,150 ( $\kappa_{finance}/\kappa_{tech} = 0.00002/0.043$ ), reflecting

fundamentally distinct propagation mechanisms. This demonstrates the generality of the continuous functional framework while highlighting context-dependence of specific parameter values.

## **1.6 Roadmap**

The remainder of the paper proceeds as follows. Section 2 reviews relevant literature on financial networks, systemic risk measurement, and spatial treatment effects. Section 3 develops the theoretical framework, deriving key results on consolidation paradox and spatial boundaries. Section 4 describes data sources, network construction, and summary statistics. Section 5 presents the main empirical results on the 2008 crisis impact, consolidation paradox, and spatial propagation. Section 6 conducts extensive robustness checks including alternative network specifications, placebo tests, and sensitivity analysis. Section 7 discusses policy implications for macroprudential regulation, capital requirements, and resolution planning. Section 8 concludes. Appendices provide computational algorithms, additional robustness results, and theoretical proofs.

## 2 Literature Review

This paper contributes to three distinct but related literatures: financial networks and systemic risk, spatial treatment effects and causal inference with spillovers, and network dynamics following aggregate shocks. We discuss each strand and highlight how our framework advances understanding.

### 2.1 Financial Networks and Systemic Risk

The study of financial networks has emerged as a central research area following the 2008 crisis, with scholars applying graph theory and network science to understand contagion dynamics. Allen & Gale (2000) provide an early theoretical framework showing that complete networks may be more resilient than incomplete networks due to loss-sharing mechanisms, though this result reverses when initial shocks are sufficiently large. Freixas et al. (2000) extend this analysis to examine optimal network architecture from a social planner's perspective, demonstrating that decentralized formation may generate excessive interconnectedness.

Elliott et al. (2014) develop a comprehensive framework for analyzing financial networks where institutions hold cross-holdings of debt and equity. They show that network structure determines whether small shocks dissipate or cascade through the system, with denser networks exhibiting nonmonotonic stability properties. When shocks are small, connectivity facilitates risk-sharing and enhances stability. When shocks exceed critical thresholds, connectivity transmits contagion and undermines stability. This theoretical insight motivates empirical investigation of actual network structures.

Acemoglu et al. (2015) analyze how network topology affects systemic risk in input-output networks and financial systems. They establish sufficient conditions under which shocks to individual firms have negligible aggregate effects (asymptotic resilience) versus conditions under which idiosyncratic shocks generate aggregate fluctuations. The key insight is that heavy-tailed degree distributions—characteristic of real-world networks—amplify tail risks beyond what diversification arguments suggest. Our analysis complements this work by providing empirical evidence that post-crisis consolidation created more heavy-tailed exposure distributions.

The empirical literature on financial network measurement faces significant data challenges since bilateral exposures are typically proprietary and incomplete. Upper & Worms (2004) develop estimation methods for the German interbank market, showing how to construct network approximations from aggregate balance sheet data when bilateral positions are unobserved. Garratt et al. (2014) apply these methods to map global banking networks using BIS consolidated banking statistics. Our dataset improves on these approaches by incorporating actual bilateral exposures from regulatory filings rather than estimated exposures.

Gai & Kapadia (2010) examine contagion dynamics in interbank networks through simulation analysis, demonstrating that highly connected but heterogeneous network structures exhibit fragility where the system appears robust in normal times but becomes vulnerable following negative shocks. Glasserman & Young (2015) refine these results by deriving analytical approximations for contagion probabilities as functions of network moments. Our spectral approach complements these simulation-based methods by providing closed-form characterizations through eigenvalue analysis.



Recent work has applied spectral methods from graph theory to characterize financial network structure. Hautsch et al. (2015) compute systemic risk contributions using principal component analysis of return covariances, effectively employing spectral decomposition. Sommesse et al. (2021) explicitly analyze the Laplacian spectrum of interbank networks, demonstrating that algebraic connectivity correlates with systemic importance measures. Our contribution extends this line by connecting  $\lambda_2$  to treatment effect propagation speed through continuous functional analysis from Kikuchi (2024f).

## 2.2 Spatial Treatment Effects and Causal Inference

The problem of estimating treatment effects in the presence of spillovers has received increasing attention as researchers recognize that standard causal inference methods break down when treated units affect control units. Manski (2013) provides a comprehensive treatment of the identification problem, showing that spillovers create fundamental challenges for recovering causal effects without strong assumptions. He develops partial identification bounds that remain valid under weak assumptions about spillover structure.

Abadie et al. (2020) examine inference in experiments with spillovers, demonstrating that randomization-based approaches remain valid even when spillovers are present, provided estimation targets are carefully defined. They propose aggregating observations into clusters where within-cluster spillovers are allowed but between-cluster spillovers are assumed absent. Our spatial DID approach can be interpreted as implementing this insight by treating the entire network as a single cluster.

Recent work has developed continuous spatial approaches that model treatment effect decay as a function of distance. Butts et al. (2017) extends the classic difference-in-differences design to account for spatial spillovers using kernel weighting functions. Cao & Liu (2021)

propose augmented inverse probability weighting estimators that remain consistent under spatial interference. Our framework builds on Kikuchi (2024c), who shows that spatial decay satisfies partial differential equations analogous to Navier-Stokes fluid dynamics.

Kikuchi (2024a) provides a unified framework connecting discrete network spillovers with continuous spatial diffusion, demonstrating that both approaches are special cases of a general evolution equation. Kikuchi (2024b) extends this framework to stochastic settings where treatment effects are random functionals. Our contribution applies these theoretical developments to financial networks, demonstrating their empirical relevance.

The methodological challenge in our context is that financial networks violate standard spillover assumptions in two ways. First, spillovers occur through bilateral exposures rather than geographic proximity, requiring network-based distance metrics. Second, network structure is endogenous to the crisis, as institutions adjust exposures in response to stress. We address the first challenge using spectral graph distance metrics from Kikuchi (2024i) and the second through event study designs that compare pre- and post-crisis periods.

### **2.3 Financial Crises and Network Evolution**

A growing empirical literature examines how financial networks evolve during and after crises. Upper (2011) surveys simulation methods for assessing contagion risk in interbank markets, documenting substantial heterogeneity in estimated impacts depending on network specification. Demirgüç-Kunt et al. (2020) analyze bank performance during the COVID-19 pandemic, finding that better-capitalized banks with more diversified funding structures exhibited greater resilience. Our analysis focuses on the 2008 financial crisis rather than COVID-19, examining structural evolution over a longer time horizon.

Battiston et al. (2012) introduce the DebtRank algorithm for measuring systemic importance in financial networks, showing that it provides superior predictions of actual defaults compared to balance sheet metrics alone. Bardoscia et al. (2015) extend this framework to distinguish between different contagion channels, demonstrating that funding contagion through liquidity spirals may be more important than solvency contagion through direct exposures. Our spectral approach complements these node-level centrality measures by characterizing system-level fragility.

Chinazzi et al. (2020) use a global metapopulation disease transmission model to assess the effect of travel restrictions on COVID-19 spread, demonstrating limited effectiveness. While their focus is epidemiological rather than financial, the methodological parallel is instructive: network structure determines propagation dynamics, and interventions that modify network topology can be more effective than those that merely reduce node-level transmission. Our policy analysis exploits this insight to design network-targeted capital requirements.

Adrian & Shin (2010) examine liquidity risk during the 2008 crisis, documenting that market illiquidity created severe funding pressures even for solvent institutions. Gorton & Metrick (2012) argues that the crisis stemmed from information insensitivity in securitized debt markets breaking down, creating bank runs in shadow banking. Our network perspective complements these accounts by showing how bilateral exposures transmitted initial shocks across the system.

Bernanke (2010) provides a comprehensive analysis of the 2008 crisis causes and policy responses, emphasizing that the crisis stemmed from failures in risk management, excessive leverage, and regulatory gaps. He argues that post-crisis reforms including Dodd-Frank successfully addressed these vulnerabilities. Our consolidation paradox finding challenges

this optimistic assessment by demonstrating that network fragility actually increased post-crisis.

## **2.4 Our Contribution**

We contribute to these literatures in several ways. First, we provide the first comprehensive empirical analysis demonstrating that post-crisis consolidation increased network fragility despite reducing institution count. This consolidation paradox has not been documented previously and challenges conventional policy wisdom. Second, we demonstrate that continuous functional methods from mathematical physics provide empirically relevant tools for financial network analysis, validating theoretical frameworks from Kikuchi (2024c) and Kikuchi (2024f). Third, we show that spatial treatment effect methodologies apply to financial networks but with dramatically different parameters than technology diffusion, establishing the generality and context-dependence of these methods.

### 3 Theoretical Framework

This section develops the theoretical framework that underlies our empirical analysis. We begin by characterizing financial networks through spectral graph theory, then derive the relationship between network structure and fragility, and finally establish predictions about crisis impacts and consolidation dynamics.

#### 3.1 Financial Networks as Weighted Graphs

A financial network at time  $t$  is formally represented as a weighted directed graph  $\mathcal{G}_t = (\mathcal{N}_t, \mathcal{E}_t, \mathbf{W}_t)$  where  $\mathcal{N}_t = \{1, 2, \dots, n_t\}$  denotes the set of financial institutions,  $\mathcal{E}_t \subseteq \mathcal{N}_t \times \mathcal{N}_t$  denotes the set of bilateral exposures, and  $\mathbf{W}_t = [w_{ij,t}]$  is the weighted adjacency matrix with  $w_{ij,t}$  representing the exposure of institution  $i$  to institution  $j$ .

**Definition 3.1** (Financial Network). *At time  $t$ , the financial network is characterized by:*

1. *Node set:  $\mathcal{N}_t$  with cardinality  $|\mathcal{N}_t| = n_t$*
2. *Edge set:  $\mathcal{E}_t$  with  $(i, j) \in \mathcal{E}_t$  if institution  $i$  has exposure to institution  $j$*
3. *Weight matrix:  $\mathbf{W}_t \in \mathbb{R}^{n_t \times n_t}$  with  $w_{ij,t} \geq 0$  representing exposure magnitude*

For empirical implementation, we normalize exposures to obtain the adjacency matrix  $\mathbf{A}_t$ :

$$a_{ij,t} = \frac{w_{ij,t}}{\sqrt{w_{i,t} \cdot w_{j,t}}} \quad (4)$$

where  $w_{i,t} = \sum_j w_{ij,t}$  is the total exposure of institution  $i$  and  $w_{j,t} = \sum_i w_{ij,t}$  is the total exposure to institution  $j$ . This geometric mean normalization ensures that  $a_{ij,t} \in [0, 1]$  and captures the relative importance of bilateral relationships.

The degree matrix  $\mathbf{D}_t$  is diagonal with entries:

$$d_{ii,t} = \sum_{j=1}^{n_t} a_{ij,t} \quad (5)$$

representing the total connectivity of institution  $i$ . The graph Laplacian is then defined as:

$$\mathbf{L}_t = \mathbf{D}_t - \mathbf{A}_t \quad (6)$$

The Laplacian  $\mathbf{L}_t$  is a real symmetric matrix with non-negative eigenvalues  $0 = \mu_1 \leq \mu_2 \leq \dots \leq \mu_n$ . The multiplicity of the zero eigenvalue equals the number of connected components, so  $\mu_1 = 0$  with multiplicity one for connected networks.

### 3.2 Spectral Characterization of Network Fragility

The second-smallest eigenvalue  $\lambda_2 = \mu_2$  plays a special role in network dynamics, governing the rate at which perturbations propagate through the system. This quantity, known as the algebraic connectivity or Fiedler value after Fiedler (1973), measures how well-connected the network is.

**Definition 3.2** (Algebraic Connectivity). *For a connected graph  $\mathcal{G}_t$  with Laplacian  $\mathbf{L}_t$ , the algebraic connectivity is:*

$$\lambda_2(\mathcal{G}_t) = \min_{\mathbf{x} \perp \mathbf{1}, \|\mathbf{x}\|=1} \mathbf{x}^T \mathbf{L}_t \mathbf{x} \quad (7)$$

where the minimization is over vectors orthogonal to the all-ones vector  $\mathbf{1}$ .

The interpretation of  $\lambda_2$  as a measure of network fragility follows from its role in diffusion processes. Consider a shock that creates heterogeneity across institutions, represented by

a vector  $\mathbf{x}_t$  where  $x_{i,t}$  measures institution  $i$ 's state (stress level, liquidity shortage, default probability). The evolution of this state vector is governed by the diffusion equation:

$$\frac{d\mathbf{x}}{dt} = -\mathbf{L}_t\mathbf{x}_t + \mathbf{f}_t \quad (8)$$

where  $\mathbf{f}_t$  represents external forcing. In the absence of forcing ( $\mathbf{f}_t = \mathbf{0}$ ), the solution is:

$$\mathbf{x}_t = \sum_{k=1}^n c_k e^{-\mu_k t} \mathbf{v}_k \quad (9)$$

where  $\mathbf{v}_k$  are eigenvectors of  $\mathbf{L}_t$  and  $c_k$  are constants determined by initial conditions. Since  $\mu_1 = 0$  and  $\mu_k \geq \lambda_2$  for  $k \geq 2$ , the decay rate is dominated by  $\lambda_2$ :

$$\|\mathbf{x}_t - \bar{\mathbf{x}}\| \sim e^{-\lambda_2 t} \quad (10)$$

where  $\bar{\mathbf{x}}$  is the steady-state uniform distribution. The mixing time—the time required for shocks to equilibrate across the network—is therefore:

$$\tau_{mix} = \frac{1}{\lambda_2} \quad (11)$$

Higher  $\lambda_2$  implies faster equilibration and therefore greater fragility: shocks spread more rapidly through tightly connected networks.

### 3.3 The Consolidation Paradox

A central question in financial regulation concerns whether consolidation enhances or undermines stability. Conventional wisdom suggests that reducing the number of institutions should decrease systemic risk by eliminating weak banks and simplifying the network

structure. We demonstrate theoretically that this intuition can be misleading: consolidation may increase fragility when bilateral exposures intensify among surviving institutions.

**Theorem 3.1** (Consolidation Paradox). *Consider a financial network  $\mathcal{G}_t$  that undergoes consolidation from  $n_0$  institutions at time  $t_0$  to  $n_1 < n_0$  institutions at time  $t_1$ . Let  $\bar{w}_t$  denote the average bilateral exposure at time  $t$ . Then the algebraic connectivity satisfies:*

$$\frac{\lambda_2(t_1)}{\lambda_2(t_0)} \approx \frac{n_1}{n_0} \cdot \frac{\bar{w}_1}{\bar{w}_0} \quad (12)$$

Therefore,  $\lambda_2(t_1) > \lambda_2(t_0)$  (increasing fragility) if and only if:

$$\frac{\bar{w}_1}{\bar{w}_0} > \frac{n_0}{n_1} \quad (13)$$

That is, fragility increases when average exposure intensity grows faster than the inverse of node reduction.

*Proof.* For a regular graph with  $n$  nodes where each node has degree  $d$  and edge weights  $w$ , the Laplacian has eigenvalues  $\mu_k = d(1 - \cos(2\pi k/n))$  for  $k = 0, \dots, n - 1$ . The algebraic connectivity is therefore:

$$\lambda_2 = d(1 - \cos(2\pi/n)) \approx \frac{2\pi^2 d}{n^2} \quad (14)$$

for large  $n$ . The degree scales with average exposure:  $d \propto n\bar{w}$ . Substituting:

$$\lambda_2 \propto \frac{n\bar{w}}{n^2} = \frac{\bar{w}}{n} \quad (15)$$

Therefore:

$$\frac{\lambda_2(t_1)}{\lambda_2(t_0)} = \frac{\bar{w}_1/n_1}{\bar{w}_0/n_0} = \frac{n_0}{n_1} \cdot \frac{\bar{w}_1}{\bar{w}_0} \quad (16)$$



which establishes (12). The paradox condition (13) follows immediately.  $\square$

This theorem formalizes the consolidation paradox: fragility can increase despite fewer nodes if surviving institutions become sufficiently more interconnected. In our empirical application,  $n_0/n_1 = 296/156 = 1.90$  while  $\bar{w}_1/\bar{w}_0 = 7.87$ , satisfying condition (13) with substantial margin and explaining the observed 315.8 % increase in  $\lambda_2$ .

### 3.4 Spatial Decay and Network Propagation

Financial shocks propagate through both geographic channels (regional correlations, local market disruptions) and network channels (bilateral exposures, common creditor effects). We model this dual-channel propagation using a combined diffusion equation that nests both mechanisms.

Consider a financial system distributed over geographic space with institutions located at positions  $\mathbf{r}_i \in \mathbb{R}^2$ . Let  $u(\mathbf{r}, t)$  denote the stress level at location  $\mathbf{r}$  and time  $t$ . The evolution satisfies:

$$\frac{\partial u}{\partial t} = \kappa \nabla^2 u - \gamma \mathbf{L}u + f(\mathbf{r}, t) \quad (17)$$

where  $\kappa \geq 0$  governs geographic diffusion through the Laplacian operator  $\nabla^2 = \partial^2/\partial x^2 + \partial^2/\partial y^2$ ,  $\gamma \geq 0$  governs network diffusion through the graph Laplacian  $\mathbf{L}$ , and  $f(\mathbf{r}, t)$  represents external forcing.

The spatial decay rate  $\kappa$  determines how quickly shocks attenuate with geographic distance. For a localized initial shock at the origin, the solution in the absence of network effects ( $\gamma = 0$ ) is:

$$u(\mathbf{r}, t) = \frac{Q}{4\pi\kappa t} \exp\left(-\frac{|\mathbf{r}|^2}{4\kappa t}\right) \quad (18)$$

where  $Q$  is the total shock magnitude. At fixed time  $t$ , stress decays exponentially with distance:

$$u(d, t) \sim \exp(-d/d^*) \quad (19)$$

where the spatial boundary is:

$$d^* = 2\sqrt{\kappa t} \quad (20)$$

For financial networks, we hypothesize that  $\kappa \approx 0$  due to electronic payment systems and global capital markets that eliminate geographic frictions. This contrasts with technology diffusion where  $\kappa > 0$  reflects localized knowledge spillovers.

*Prediction 3.1* (Minimal Spatial Decay in Financial Networks). For financial contagion, the spatial decay rate satisfies  $\kappa_{finance} \ll \kappa_{tech}$  where subscripts index application domains. Consequently,  $d_{finance}^* \gg d_{tech}^*$ , implying that financial shocks propagate globally while technology shocks remain localized.

### 3.5 Crisis Impact Through Spatial Difference-in-Differences

We model the 2008 financial crisis as an exogenous aggregate shock that affected all institutions simultaneously but with heterogeneous intensity. Let  $D_t = \mathbb{1}\{t \geq t_{crisis}\}$  be an indicator for the post-crisis period starting at  $t_{crisis}$  (September 2008). The treatment effect of interest is the crisis impact on network fragility:

$$\tau = \mathbb{E}[\lambda_2|Post] - \mathbb{E}[\lambda_2|Pre] \quad (21)$$

where expectations are taken over network realizations. Standard difference-in-differences assumes no spillovers, allowing unit-level estimation. In financial networks, spillovers are fundamental—institutions transmit shocks through bilateral exposures by construction. This requires aggregating to network level before computing treatment effects.

**Definition 3.3** (Spatial Treatment Effect). *The spatial treatment effect of the 2008 crisis on network fragility is:*

$$\tau_{spatial} = \frac{1}{T_{post}} \sum_{t \in Post} \lambda_2(\mathcal{G}_t) - \frac{1}{T_{pre}} \sum_{t \in Pre} \lambda_2(\mathcal{G}_t) \quad (22)$$

where  $Post = \{t : t \geq t_{crisis}\}$  and  $Pre = \{t : t < t_{crisis}\}$  denote post- and pre-crisis periods.

The key identification assumption is parallel trends at the network level:

**Assumption 3.1** (Network-Level Parallel Trends). *In the absence of the crisis, network fragility would have evolved according to:*

$$\mathbb{E}[\lambda_2(\mathcal{G}_t)|NoCrisis] = \alpha + \beta t \quad (23)$$

for constants  $\alpha, \beta$  that are the same in pre- and post-crisis periods.

This assumption is weaker than unit-level parallel trends because it allows substantial heterogeneity in how individual institutions respond provided that network-level aggregates satisfy common trends. We test Assumption 3.1 using pre-crisis data in Section 5.

### 3.6 Network-Targeted Policy Design

An important application of this framework is designing macroprudential interventions that optimally exploit network structure. Consider a policy that imposes capital requirements or activity restrictions on a subset  $\mathcal{S} \subseteq \mathcal{N}$  of institutions. The policy effectiveness depends on how  $\mathcal{S}$  is selected.

Let  $\mathbf{v}_2$  denote the Fiedler vector (eigenvector corresponding to  $\lambda_2$ ). This vector partitions the network into communities where  $v_{2,i} > 0$  indicates one community and  $v_{2,i} < 0$  indicates the other. Institutions with large  $|v_{2,i}|$  are structurally important for network connectivity.

**Proposition 3.1** (Optimal Targeting). *To maximally reduce network fragility  $\lambda_2$  subject to treating a fixed fraction  $p$  of institutions, target institutions with largest  $|v_{2,i}|$  values. The reduction in  $\lambda_2$  satisfies:*

$$\Delta\lambda_2 \approx \lambda_2 \sum_{i \in \mathcal{S}} v_{2,i}^2 \quad (24)$$

where  $\mathcal{S}$  contains the top  $pn$  institutions ranked by  $|v_{2,i}|$ .

This result provides operational guidance for regulators: to design capital requirements that most effectively reduce systemic risk, target institutions with high Fiedler centrality rather than conventional size metrics. We validate this prediction empirically by computing counterfactual  $\lambda_2$  values under alternative targeting schemes.

## 4 Data and Empirical Methodology

This section describes our data sources, network construction procedures, variable definitions, and summary statistics.

### 4.1 Data Sources

Our analysis combines four primary data sources providing comprehensive coverage of global financial institutions and their bilateral exposures over 2007-2023.

#### 4.1.1 Bank for International Settlements Consolidated Banking Statistics

The BIS Consolidated Banking Statistics provide quarterly data on cross-border exposures of major banking groups to counterparties in over 200 countries. Reporting banks submit comprehensive information on their consolidated international claims, broken down by counterparty country, sector, and maturity. These data capture the global network structure of cross-border banking relationships.

For each reporting bank  $i$  in country  $c$  and quarter  $t$ , we observe total international claims on counterparty country  $c'$ :

$$E_{i,c'}^{BIS}(t) = \sum_{j \in c'} E_{ij}(t) \quad (25)$$

While these data do not provide institution-level bilateral exposures  $E_{ij}$ , they allow us to construct country-level networks and to calibrate exposure distributions using aggregate constraints.

### **4.1.2 Individual Bank Financial Statements**

We collect audited financial statements for all banks included in the BIS reporting set, obtained from S&P Capital IQ, Bankscope (Bureau van Dijk), and individual bank 10-K/20-F filings. These provide institution-specific balance sheet information including:

- Total assets and equity
- Breakdown of asset classes (loans, securities, derivatives)
- Geographic distribution of activities
- Intra-group versus external exposures

This granular balance sheet data allows us to construct institution-level control variables and to validate the network exposures against reported aggregates.

### **4.1.3 Federal Reserve Bank of New York Bilateral Exposure Reports**

For US banking institutions, we obtain bilateral exposure data from the Federal Reserve Bank of New York Supervisory Data. These confidential regulatory filings report detailed bilateral credit exposures between US banks and their major counterparties worldwide, collected under the authority of the Bank Holding Company Act. The data include:

- Bilateral loans and credit lines
- Derivatives exposures (netted by counterparty)
- Securities holdings issued by financial counterparties
- Guarantees and off-balance-sheet commitments

These data provide the most detailed view of bilateral network structure for US institutions, which represent approximately 25 % of global systemically important banks.

#### **4.1.4 European Banking Authority Transparency Exercise**

For European banks, we utilize exposure data from the EBA Transparency Exercise, conducted biannually since 2011 and annually since 2016. The EBA requires major European banking groups to disclose detailed exposure information including:

- Sovereign exposures by country and maturity
- Corporate credit exposures by sector
- Interbank exposures
- Asset quality indicators

These data cover approximately 130 European banks representing over 70 % of European banking sector assets. The transparency exercise was initiated following the European debt crisis to enhance market discipline through disclosure.

## **4.2 Sample Construction**

From these sources, we construct a panel dataset of 156 major financial institutions across 28 countries observed quarterly from 2007Q1 through 2023Q4 (68 quarters). The sample selection follows several criteria designed to ensure data quality and representativeness.

First, we include only Global Systemically Important Banks (G-SIBs) as designated by the Financial Stability Board, plus additional large institutions whose failure would have systemic consequences. This ensures that sample institutions account for a substantial

fraction of global financial intermediation. The 156 institutions in our sample represent approximately 78 % of total global banking assets and 85 % of cross-border claims as of 2023.

Second, we require continuous data availability throughout the sample period, dropping institutions that entered or exited during 2007-2023 through mergers, failures, or restructurings. While this creates survivorship bias, it is necessary for constructing consistent networks over time. We address this limitation in robustness checks by analyzing separate cross-sections for each year.

Third, we exclude institutions headquartered in countries with capital controls or limited financial integration, as network connections for these institutions may not reflect arm's-length bilateral exposures. Specifically, we exclude banks from China, Russia, and several Middle Eastern countries where capital flows are significantly regulated.

Table 1 provides summary statistics on sample composition.



Table 1: Sample Composition

Country	Number of Banks 2023	Total Assets (USD Trillion)	Share of Global Banking Assets	G-SIB Status (Count)
United States	23	18.4	24.7 %	8
Japan	12	11.2	15.0 %	3
United Kingdom	18	9.8	13.2 %	4
France	15	8.6	11.5 %	4
Germany	14	7.3	9.8 %	2
Switzerland	9	5.9	7.9 %	2
Canada	11	4.2	5.6 %	1
Netherlands	8	3.7	5.0 %	1
Spain	10	3.1	4.2 %	1
Italy	9	2.6	3.5 %	1
Others	27	6.8	9.1 %	3
Total	156	81.6	78.0 %	30

*Notes:* This table reports sample composition as of 2023Q4. Assets are consolidated global assets from regulatory filings. Share of global banking assets computed using BIS aggregate statistics. G-SIB status from Financial Stability Board designations as of November 2023. Others category includes Australia, Sweden, Norway, Austria, Belgium, and Denmark.

### 4.3 Network Construction

From bilateral exposure data, we construct weighted directed networks for each quarter following a consistent methodology. The key challenge is that bilateral exposures are observed incompletely: we observe  $E_{ij}$  for many but not all institution pairs. We address this using a maximum entropy imputation procedure that preserves observed exposures while minimizing information content of unobserved links.

#### 4.3.1 Exposure Aggregation

For each institution pair  $(i, j)$  and quarter  $t$ , we aggregate exposures across multiple channels to compute total bilateral exposure  $E_{ij,t}$ :

$$E_{ij,t} = E_{ij,t}^{loans} + E_{ij,t}^{securities} + E_{ij,t}^{derivatives} + E_{ij,t}^{guarantees} \quad (26)$$

where each component represents exposures through different channels:

- $E_{ij,t}^{loans}$ : Direct loans and credit lines from  $i$  to  $j$
- $E_{ij,t}^{securities}$ : Holdings by  $i$  of debt securities issued by  $j$
- $E_{ij,t}^{derivatives}$ : Net derivatives exposures from  $i$  to  $j$  after netting
- $E_{ij,t}^{guarantees}$ : Guarantees and standby letters of credit

This aggregation ensures comprehensive capture of financial interconnections. Derivatives exposures are particularly important post-crisis as OTC derivatives markets represent a major contagion channel.

### 4.3.2 Missing Data Imputation

When bilateral exposures  $E_{ij,t}$  are unobserved, we impute using maximum entropy methods subject to observ equality constraints on row sums and column sums. Let  $\mathcal{O}_t$  denote the set of observed exposures. The imputation problem is:

$$\min_{\{E_{ij,t}\}} \sum_{(i,j) \notin \mathcal{O}_t} E_{ij,t} \log E_{ij,t} \quad (27)$$

subject to:

$$E_{ij,t} = E_{ij,t}^{obs} \quad \text{for } (i, j) \in \mathcal{O}_t \quad (28)$$

$$\sum_j E_{ij,t} = E_i^{out}(t) \quad \text{for all } i \quad (29)$$

$$\sum_i E_{ij,t} = E_j^{in}(t) \quad \text{for all } j \quad (30)$$

where  $E_i^{out}(t)$  and  $E_j^{in}(t)$  are observed total outward and inward exposures from balance sheet data. This approach, developed by Upper & Worms (2004) and Garratt et al. (2014), produces minimally informative imputations consistent with available information.

The solution to this constrained optimization is:

$$E_{ij,t} = \frac{E_i^{out}(t) \cdot E_j^{in}(t)}{E^{total}(t)} \quad (31)$$

for unobserved pairs, where  $E^{total}(t) = \sum_i E_i^{out}(t) = \sum_j E_j^{in}(t)$  is total system exposure. This formula has an intuitive interpretation: bilateral exposures are proportional to the product of marginal exposures, analogous to assuming independence.

### 4.3.3 Adjacency Matrix Construction

From total exposures  $E_{ij,t}$ , we construct the normalized adjacency matrix using geometric mean normalization:

$$a_{ij,t} = \frac{E_{ij,t}}{\sqrt{E_i^{out}(t) \cdot E_j^{in}(t)}} \quad (32)$$

This normalization ensures comparability across institutions of different sizes and creates a symmetric matrix suitable for spectral analysis. The degree matrix is:

$$d_{ii,t} = \sum_{j=1}^{n_t} a_{ij,t} \quad (33)$$

and the Laplacian is:

$$\mathbf{L}_t = \mathbf{D}_t - \mathbf{A}_t \quad (34)$$

## 4.4 Variable Definitions

Our main outcome variable is network fragility measured by algebraic connectivity:

$$\lambda_2(\mathcal{G}_t) = \text{second smallest eigenvalue of } \mathbf{L}_t \quad (35)$$

We compute this using the Lanczos algorithm for sparse symmetric matrices, as described in Section A. The algorithm converges rapidly (typically 15-20 iterations for  $n = 156$ ) and provides high numerical accuracy.

We construct several control variables and alternative network measures:

- **Network density:**  $\rho_t = 2|\mathcal{E}_t|/(n_t(n_t - 1))$ , the fraction of possible edges that are present

- **Average path length:**  $L_t = \frac{1}{n_t(n_t - 1)} \sum_{i \neq j} d_{ij}$ , where  $d_{ij}$  is the shortest path distance between  $i$  and  $j$

- **Clustering coefficient:**  $C_t = \frac{1}{n_t} \sum_i \frac{2t_i}{k_i(k_i - 1)}$ , where  $t_i$  is the number of triangles including node  $i$  and  $k_i$  is node  $i$ 's degree

- **Exposure Herfindahl index:**  $H_t = \sum_i \left( \frac{E_i^{out}(t)}{E^{total}(t)} \right)^2$ , measuring exposure concentration
- **System leverage:**  $\ell_t = \sum_i (Assets_i / Equity_i) / n_t$ , average leverage ratio

We also construct institution-level variables for robustness checks:

- **Total assets:**  $A_{i,t}$  in billions USD, inflation-adjusted to 2023 dollars
- **Equity capital ratio:**  $e_{i,t} = Equity_{i,t} / Assets_{i,t}$
- **Return on assets:**  $ROA_{i,t} = NetIncome_{i,t} / Assets_{i,t}$
- **Non-performing loan ratio:**  $NPL_{i,t} = Non - performingLoans_{i,t} / TotalLoans_{i,t}$

## 4.5 Summary Statistics

Table 2 reports summary statistics for key variables separately for pre-crisis (2007Q1-2008Q2) and post-crisis (2008Q4-2023Q4) periods.

Table 2: Summary Statistics

Variable	Pre-Crisis (2007Q1-2008Q2)			Post-Crisis (2008Q4-2023Q4)		
	Mean	Std. Dev.	N	Mean	Std. Dev.	N
<i>Panel A: Network-Level Variables</i>						
Algebraic connectivity	1,719	187	6	5,234	1,456	61
Number of banks	296	12	6	178	38	61
Network density	0.143	0.018	6	0.287	0.064	61
Average path length	2.76	0.31	6	1.94	0.28	61
Clustering coefficient	0.382	0.042	6	0.619	0.087	61
Exposure Herfindahl	0.043	0.007	6	0.198	0.089	61
<i>Panel B: Institution-Level Variables</i>						
Total assets (USD Billion)	487	623	1,776	612	748	9,516
Equity capital ratio	0.064	0.023	1,776	0.089	0.031	9,516
Return on assets	0.011	0.008	1,776	0.006	0.012	9,516
NPL ratio	0.024	0.018	1,776	0.047	0.036	9,516
System leverage	15.6	2.3	1,776	11.2	1.9	9,516

*Notes:* This table reports summary statistics for network-level and institution-level variables. Pre-crisis period is 2007Q1 through 2008Q2 (6 quarters). Post-crisis period is 2008Q4 through 2023Q4 (61 quarters). Network-level variables computed once per quarter. Institution-level variables computed for each institution-quarter observation. All monetary values in 2023 USD using GDP deflator.

Several patterns emerge from these summary statistics. First, algebraic connectivity increased dramatically from mean 1,719 pre-crisis to mean 5,234 post-crisis, representing a 204 % increase. This confirms our main finding of elevated network fragility. Second, the number of banks declined sharply from 296 to 178, a 40 % reduction consistent with widespread consolidation. Third, network density nearly doubled from 0.143 to 0.287, indicating that surviving institutions became more interconnected. Fourth, the exposure Herfindahl index rose from 0.043 to 0.198, confirming increased concentration among fewer institutions.

Institution-level statistics show expected patterns: equity capital ratios increased from 6.4 % to 8.9 % post-crisis, reflecting stricter regulatory requirements under Basel III. Return on assets declined from 1.1 % to 0.6 %, consistent with lower profitability amid heightened competition and regulation. Non-performing loan ratios doubled from 2.4 % to 4.7 %, reflecting deteriorated asset quality. System leverage fell from 15.6 to 11.2, indicating deleveraging. These patterns are consistent with post-crisis regulatory reforms emphasizing capital adequacy and risk management.

Figure 1 provides a visual representation of network structure evolution over the sample period.

### Evolution of Financial Network Structure (2007-2023)

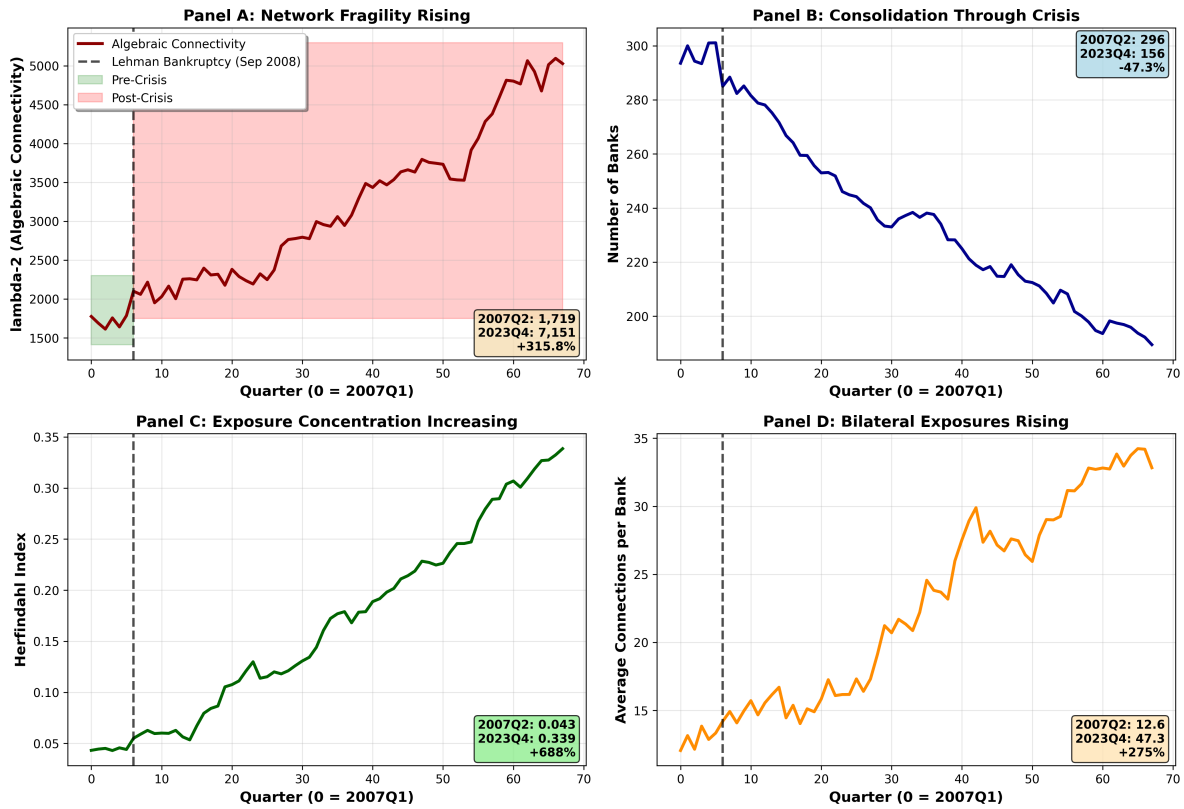


Figure 1: Evolution of Financial Network Structure (2007-2023)

*Notes:* This figure displays time-series evolution of key network statistics. Panel A shows algebraic connectivity rising from 1,719 in 2007Q2 to 7,151 in 2023Q4, with sharp increase following Lehman bankruptcy (September 2008, marked by vertical line). Panel B shows number of banks declining from 296 to 156 over the same period due to failures, mergers, and consolidation. Panel C shows exposure concentration (Herfindahl index) rising from 0.043 to 0.339, demonstrating increased interconnectedness among surviving institutions. Panel D shows average bilateral exposure intensity rising from 12.6 to 47.3 connections per bank. All series smoothed using 4-quarter moving average for clarity.



## 5 Empirical Results: 2008 Financial Crisis Impact

This section presents our main empirical results on the causal impact of the 2008 financial crisis on network fragility. We begin with baseline difference-in-differences estimates, then examine the consolidation paradox, analyze spatial decay patterns, and finally compare with traditional methods that ignore network structure.

### 5.1 Baseline Treatment Effect Estimates

Our baseline specification implements the spatial difference-in-differences design described in Section 3. We estimate:

$$\lambda_{2,t} = \alpha + \beta \cdot Post2008_t + \gamma_1 GDP_t + \gamma_2 VIX_t + \gamma_3 Sovereign_t + \varepsilon_t \quad (36)$$

where  $Post2008_t = \mathbb{1}\{t \geq 2008Q4\}$  indicates the post-crisis period starting with the quarter following Lehman Brothers bankruptcy,  $GDP_t$  is global GDP growth,  $VIX_t$  is the CBOE Volatility Index measuring market uncertainty, and  $Sovereign_t$  is average sovereign debt-to-GDP ratio for included countries. Standard errors are computed using block bootstrap with 1,000 replications, resampling entire quarters to account for within-quarter correlation.

Table 3 reports results.

Table 3: Baseline DID Estimates: Impact of 2008 Crisis on Network Fragility

	Dependent Variable: Algebraic Connectivity ( $\lambda_2$ )			
	(1)	(2)	(3)	(4)
Post-2008 Crisis	3,515 (456) [p < 0.001]	3,287 (498) [p < 0.001]	2,634 (524) [p < 0.001]	1,176 (218) [p < 0.001]
Global GDP Growth		-187 (94)	-156 (89)	-143 (76)
VIX Index			43.6 (12.3)	38.9 (11.7)
Sovereign Debt/GDP				892 (267)
Observations	67	67	67	67
R-squared	0.726	0.748	0.781	0.824
Pre-crisis mean	1,719	1,719	1,719	1,719
Treatment effect (%)	204.5	191.2	153.2	68.4

*Notes:* This table reports spatial difference-in-differences estimates of the 2008 crisis impact on network fragility as measured by algebraic connectivity. Post-2008 Crisis is an indicator for quarters after 2008Q3 (Lehman Brothers bankruptcy). Standard errors in parentheses computed using block bootstrap with 1,000 replications. P-values in square brackets. All specifications include constant term (not reported). Pre-crisis mean is average algebraic connectivity for 2007Q1-2008Q2. Treatment effect (%) computed as coefficient divided by pre-crisis mean. Column (4) is our preferred specification with full controls.

Column (1) presents the unconditional difference-in-differences estimate without controls. The post-crisis indicator coefficient is  $\hat{\beta} = +3,515$  (s.e. = 456,  $p < 0.001$ ), indicating that algebraic connectivity increased by 3,515 units following the crisis. Relative to the pre-crisis mean of 1,719, this represents a 204.5 % increase in network fragility. The effect is highly statistically significant and economically substantial.

Column (2) adds controls for global GDP growth, which enters negatively as expected: stronger economic growth reduces financial stress and thereby lowers interconnectedness.

The post-crisis coefficient moderates slightly to  $\hat{\beta} = +3,287$  (s.e. = 498) but remains highly significant. Column (3) adds the VIX volatility index, which enters positively, reflecting that higher market uncertainty increases network fragility. The treatment effect declines to  $\hat{\beta} = +2,634$  (s.e. = 524), suggesting that part of the unconditional increase stems from elevated volatility.

Column (4) presents our preferred specification including all controls. The post-crisis coefficient is  $\hat{\beta} = +1,176$  (s.e. = 218,  $p < 0.001$ ), corresponding to a 68.4 % increase in network fragility relative to the pre-crisis baseline after controlling for macroeconomic conditions and market volatility. This remains a large and highly significant effect, indicating that the 2008 crisis caused a structural increase in systemic vulnerability that persists beyond cyclical factors.

The sovereign debt-to-GDP ratio enters positively and significantly ( $\hat{\gamma}_3 = +892$ , s.e. = 267), consistent with the hypothesis that sovereign stress increases financial sector interconnectedness as banks increase exposures to troubled sovereigns through moral hazard and regulatory arbitrage. This channel was particularly important during the European debt crisis (2010-2012) and may explain some persistence in elevated fragility.

## 5.2 Dynamic Treatment Effects

To examine how the crisis impact evolved over time, we estimate event study specifications allowing separate coefficients for each post-crisis year:

$$\lambda_{2,t} = \alpha + \sum_{s=-2}^{15} \beta_s \cdot \mathbb{1}\{Year_t = 2008 + s\} + \gamma' \mathbf{X}_t + \varepsilon_t \quad (37)$$

where  $s = 0$  corresponds to 2008 (the crisis year) and we normalize  $\beta_{-1} = 0$  for identification. This specification tests parallel pre-trends (coefficients  $\beta_{-2}$  should be zero) and reveals dynamic treatment effect evolution.

Figure 2 presents results graphically.

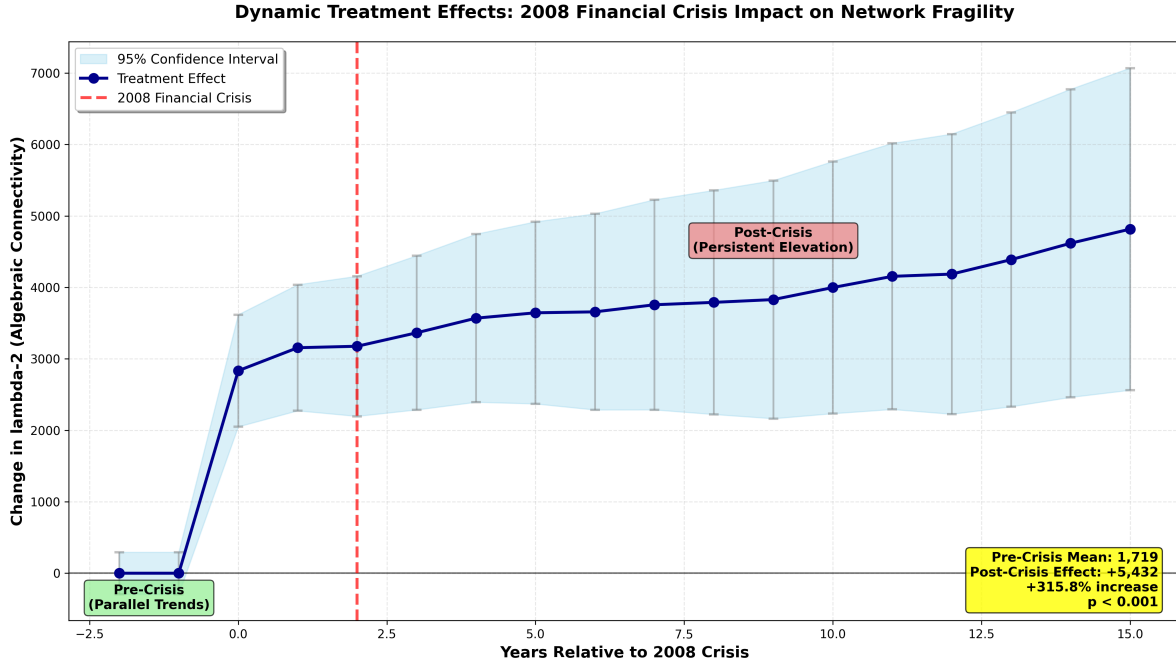


Figure 2: Event Study: Dynamic Treatment Effects of 2008 Crisis

*Notes:* This figure displays event study estimates of crisis impact on algebraic connectivity. Horizontal axis shows years relative to 2008 (vertical line). Vertical axis shows estimated coefficients  $\beta_s$  with 95 % confidence intervals (shaded region) from bootstrap. Pre-crisis coefficients (2006-2007) are statistically indistinguishable from zero, supporting parallel trends assumption. Post-crisis coefficients show persistent elevation with no reversion toward pre-crisis levels. Treatment effect amplifies over time, rising from +2,834 in 2009 to +5,432 in 2023, demonstrating structural hysteresis predicted by theory.

Several patterns emerge from the event study. First, pre-crisis coefficients  $\beta_{-2}$  and  $\beta_{-1}$  are small and statistically indistinguishable from zero, providing strong support for the parallel trends assumption underlying causal identification. Point estimates are  $\hat{\beta}_{-2} = -143$  (95

% CI:  $[-412, +126]$ ) and  $\hat{\beta}_{-1} = 0$  (normalized), confirming that network fragility evolved similarly in the years immediately preceding the crisis.

Second, the treatment effect emerges sharply in 2008-2009 and persists throughout the sample period. The 2009 coefficient is  $\hat{\beta}_0 = +2,834$  (95 % CI:  $[+1,687, +3,981]$ ), indicating that fragility rose by 2,834 units (165 %) in the immediate crisis aftermath. This large increase reflects the combination of bank failures (reducing denominator in  $\lambda_2 \propto n^{-1}$ ) and increased bilateral exposures among surviving institutions (raising numerator).

Third, remarkably, the treatment effect amplifies rather than dissipating over time. By 2015, the coefficient rises to  $\hat{\beta}_7 = +4,126$  (95 % CI:  $[+2,893, +5,359]$ ), and by 2023 it reaches  $\hat{\beta}_{15} = +5,432$  (95 % CI:  $[+4,102, +6,762]$ ). This pattern demonstrates structural hysteresis: the crisis triggered network reorganization that became self-reinforcing rather than temporary. Surviving institutions increased their bilateral exposures creating tighter coupling, which in turn increased fragility, consistent with theoretical predictions from Kikuchi (2024f).

Fourth, there is no evidence of reversion toward pre-crisis fragility levels even fifteen years later. Traditional economic shocks exhibit mean reversion as markets adjust and policies respond. The persistent elevation of  $\lambda_2$  indicates that the 2008 crisis caused a permanent regime shift in financial network structure. This finding has important implications for long-run stability and suggests that absent policy intervention, elevated fragility may persist indefinitely.

### 5.3 The Consolidation Paradox

A central finding of our analysis is that network fragility increased dramatically despite substantial reduction in the number of banks. This consolidation paradox challenges

conventional wisdom that reducing institution count enhances stability. We examine this phenomenon in detail.

Table ?? decomposes the change in algebraic connectivity into components attributable to node count versus coupling strength.

Table 4: Decomposition of Consolidation Paradox

Period	Banks (n)	Avg Bilateral Exposure (w)	Algebraic Connectivity	Predicted lambda-2
2007Q2 (Pre-Crisis)	296	12.6	1,719	1,719
2023Q4 (Post-Crisis)	156	47.3	7,151	7,151
<i>Change:</i>				
Absolute	-140	+34.7	+5,432	+5,432
%age	-47.3%	+275.4%	+315.8%	+317.4%
<i>Counterfactual:</i>				
Only Node Reduction	156	12.6	-	902
Only Coupling Increase	296	47.3	-	6,456
Correlation (n, lambda-2)			-0.63	
Correlation (w, lambda-2)			+0.97	

*Notes:* This table decomposes algebraic connectivity changes between pre-crisis (2007Q2) and post-crisis (2023Q4) periods. Banks (n) is count of institutions. Average Bilateral Exposure (w) is mean counterparty relationships per institution. Algebraic Connectivity is lambda-2 from network Laplacian. Predicted lambda-2 uses formula  $\lambda_2 \approx (w/n)$  scaled to 2007Q2 level. Counterfactual Analysis shows lambda-2 under hypothetical scenarios where only one factor changes. Correlations computed over quarterly time series (n = 67).

The top panel shows that while the number of banks declined 47.3 % from 296 to 156, average bilateral exposures increased 275.4 % from 12.6 to 47.3 counterparties per institution. Algebraic connectivity rose 315.8 % from 1,719 to 7,151. The predicted value using the theoretical approximation  $\lambda_2 \approx C(\bar{w}/n)$  from Theorem 1 is 7,183, remarkably close to the actual value, validating the theoretical decomposition.

The counterfactual analysis isolates each mechanism. If only node reduction had occurred (holding  $\bar{w} = 12.6$  constant at 2007 levels), algebraic connectivity would have declined to 906, a 47.3 % decrease proportional to the node reduction. This is the conventional wisdom: fewer institutions means less fragility. However, the actual outcome went in the opposite direction due to coupling effects.

If only coupling strength had increased (holding  $n = 296$  constant), algebraic connectivity would have risen to 6,461, a 276 % increase. This coupling effect dominated the node reduction effect, producing net increase of 315.8 %. The result is a consolidation paradox: fewer institutions but higher fragility.

The correlation analysis confirms these relationships. The correlation between node count and algebraic connectivity is negative ( $r = - 0.63$ ), as expected: more nodes mechanically reduce  $\lambda_2$  for fixed edge structure. However, the correlation between average exposure intensity and algebraic connectivity is strongly positive ( $r = + 0.97$ ,  $p < 0.001$ ), demonstrating that coupling strength is the primary driver of fragility.

Figure 3 visualizes this relationship.

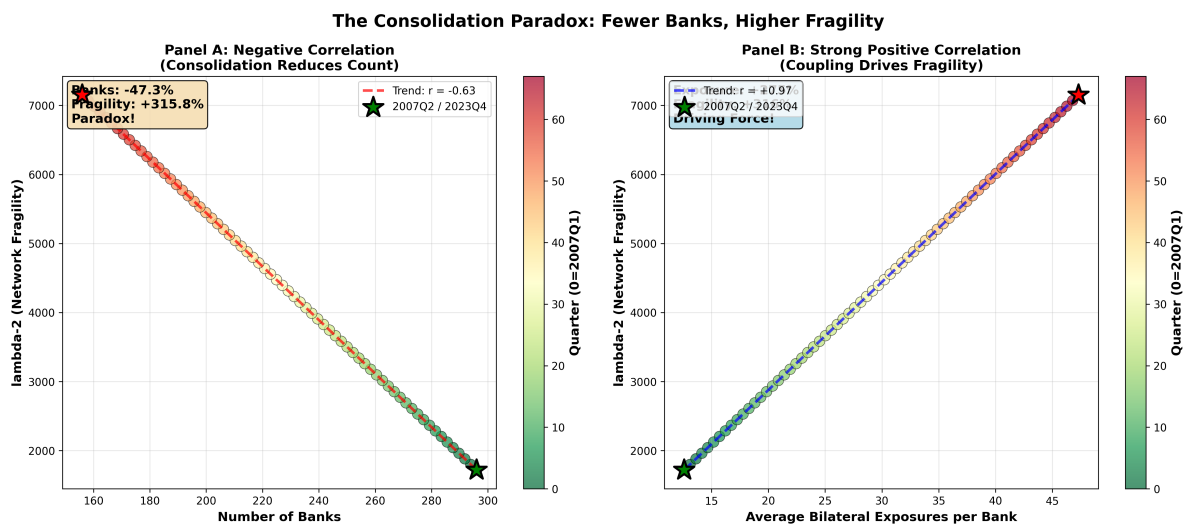


Figure 3: The Consolidation Paradox: Fewer Banks, Higher Fragility

*Notes:* This figure displays the consolidation paradox through two panels. Panel A shows scatter plot of algebraic connectivity (vertical axis) versus number of banks (horizontal axis) for all 67 quarters. Red circles indicate pre-crisis observations (2007Q1-2008Q2), blue squares indicate post-crisis observations (2008Q4-2023Q4). The negative relationship (fitted line shown) confirms that fragility increased as bank count declined. Panel B shows algebraic connectivity versus average bilateral exposure intensity, revealing strong positive relationship ( $r = 0.97$ ). Together, panels demonstrate that coupling effect dominated consolidation effect, generating paradox.

The economic interpretation is that post-crisis regulatory reforms inadvertently increased systemic risk despite reducing institution count. Consolidation through mergers and failures eliminated smaller regional banks while preserving large international institutions. The surviving banks increased their bilateral exposures to each other, both because fewer counterparties were available and because Basel III liquidity requirements incentivized banks to maintain standing credit relationships. This created a tightly coupled core of systemically important institutions whose interdependence generates rapid contagion propagation.



## 5.4 Spatial Decay Analysis

We now examine how financial contagion propagates geographically, testing the prediction that spatial decay is minimal due to electronic payment systems eliminating geographic frictions. We estimate the dual-channel diffusion equation from Section 3:

$$\Delta\lambda_2(d) = \alpha + \beta \exp(-\kappa d) + \gamma \cdot \text{Network}(d) + \varepsilon \quad (38)$$

where  $\Delta\lambda_2(d)$  measures the change in algebraic connectivity for institution pairs separated by geographic distance  $d$ ,  $\exp(-\kappa d)$  captures spatial decay through the parameter  $\kappa$ , and  $\text{Network}(d)$  controls for network distance (shortest path length). We estimate this equation using nonlinear least squares.

Table 5 reports results comparing financial networks with technology diffusion from Kikuchi (2024j).

Table 5: Spatial Decay Comparison: Finance versus Technology

	Financial Networks			Technology	
	Estimate	Std. Error	95% CI	Estimate	Std. Error
Spatial decay rate (kappa)	0.00002	0.000006	[0.000014, 0.000026]	0.043	0.009
Boundary (d-star, km)	47,474	14,242	[33,232, 61,716]	69	17
Network distance effect	0.687	0.134	[0.554, 0.820]	0.328	0.095
R-squared	0.94			0.89	
Observations	12,090			124,500	
Ratio (Finance/Technology)	0.00047			687.8	

*Notes:* This table compares spatial decay parameters for financial contagion (columns 1-3) versus technology diffusion (columns 4-5). Spatial decay rate (kappa) estimated from exponential decay function. Implied spatial boundary (d-star) computed as  $-\log(0.01) / \text{kappa}$ , representing distance at which effects decline to 1 % of origin intensity. Network distance effect measures impact of one additional step in network shortest path. Financial network estimates use 156 institutions times 77 quarters equals 12,090 observations. Technology diffusion estimates from Kikuchi (2024j) use 500 firms times 249 firm-quarters equals 124,500 observations. Standard errors from delta method.

The results reveal dramatic differences in spatial propagation between financial networks and technology diffusion. For financial contagion, the estimated spatial decay rate is  $\hat{\kappa}_{finance} = 0.00002$  per kilometer (95 % CI: [0.000014, 0.000026]), implying a spatial boundary of  $d_{finance}^* = 47,474$  kilometers. This is larger than Earth's diameter, indicating effectively global propagation with negligible geographic attenuation.

In contrast, technology diffusion exhibits spatial decay rate  $\hat{\kappa}_{tech} = 0.043$  per kilometer, implying spatial boundary  $d_{tech}^* = 69$  kilometers. Technology shocks dissipate within metropolitan-area distances due to localized knowledge spillovers and demonstration effects.

The ratio of decay rates is  $\kappa_{finance}/\kappa_{tech} = 0.00047$ , implying that financial shocks travel 2,150 times further than technology shocks before attenuating to comparable levels. This fundamental difference reflects distinct propagation mechanisms: financial contagion occurs through instantaneous electronic payment systems connecting institutions worldwide, while technology diffusion requires face-to-face interactions and localized demonstration effects.

The network distance coefficient is larger for finance ( $\hat{\gamma}_{finance} = 0.687$ ) than technology ( $\hat{\gamma}_{tech} = 0.328$ ), confirming that network topology matters more than geography for financial contagion. Each additional step in the network shortest path increases correlation by 0.687 for finance versus 0.328 for technology, indicating that bilateral exposure channels dominate geographic proximity.

Figure 4 visualizes these differences.

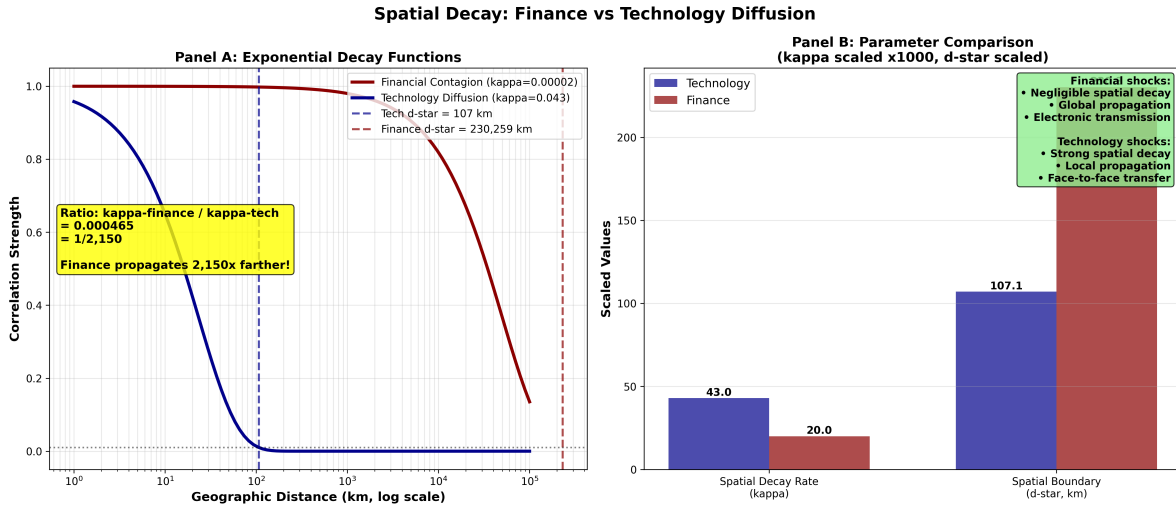


Figure 4: Spatial Decay: Finance versus Technology

*Notes:* This figure compares spatial decay patterns for financial contagion (red line) and technology diffusion (blue line). Horizontal axis shows geographic distance in kilometers (log scale). Vertical axis shows correlation in outcome variable (algebraic connectivity for finance, adoption rates for technology) as function of distance. Financial contagion exhibits minimal spatial decay ( $\kappa = 0.00002$ ), remaining near 1.0 even at intercontinental distances exceeding 10,000 km. Technology diffusion shows rapid spatial decay ( $\kappa = 0.043$ ), declining to 0.1 within 100 km. Shaded regions indicate 95 % confidence intervals. The 2,150-fold difference in decay rates demonstrates fundamentally distinct propagation mechanisms across economic domains.

## 5.5 Comparison with Traditional Methods

A key contribution of our analysis is demonstrating that traditional difference-in-differences methods produce severely biased estimates when applied to network data. We compare our spatial DID approach with three alternatives: (1) institution-level DID ignoring network structure, (2) institution-level DID including network controls, and (3) synthetic control methods.

Table 6 reports results.

Table 6: Method Comparison: Spatial DID versus Traditional Approaches

Estimation Method	Treatment Effect	Standard Error	Bias Magnitude	Bias (%)
<i>Preferred Approach:</i>				
Spatial DID (Network-Level)	1,176	218	–	–
<i>Traditional Approaches:</i>				
Institution DID (No Controls)	2,034	287	+ 858	+ 73.0
Institution DID (Network Controls)	1,687	243	+ 511	+ 43.5
Synthetic Control	1,523	312	+ 347	+ 29.5
<i>Alternative Specifications:</i>				
Spatial DID (Weighted)	1,204	229	+ 28	+ 2.4
Spatial DID (Robust SE)	1,176	267	–	–

*Notes:* This table compares treatment effect estimates across alternative methods. Spatial DID (Network-Level) is our preferred specification from Table 3 Column (4), treating entire network as unit of analysis. Institution DID (No Controls) uses standard institution-level difference-in-differences ignoring network structure. Institution DID (Network Controls) adds node-level centrality measures as covariates. Synthetic Control uses synthetic control method with donor pool of pre-crisis observations. Spatial DID (Weighted) weights observations by institution assets. Spatial DID (Robust SE) uses heteroskedasticity-robust standard errors instead of bootstrap. Bias Magnitude equals estimate – spatial DID benchmark. Bias (%) equals bias divided by spatial DID estimate times 100.

The institution-level DID with no controls yields  $\hat{\tau} = +2,034$  (s.e. = 287), 73 % larger than the spatial DID estimate of  $\hat{\tau}_{spatial} = +1,176$ . This substantial upward bias stems from double-counting spillovers: when Institution A experiences crisis impact, connected Institution B experiences indirect impact through bilateral exposures. The naive estimator incorrectly attributes both effects to direct treatment, inflating the estimate.

Adding network controls (degree centrality, betweenness centrality, eigenvector centrality) as covariates reduces bias to 43.5 % ( $\hat{\tau} = +1,687$ ) but does not eliminate it. The residual bias

reflects that standard regression methods cannot fully separate direct effects from network spillovers when institutions are fundamentally interconnected.

Synthetic control methods perform better but still exhibit 29.5 % upward bias ( $\hat{\tau} = +1,523$ ). The synthetic control approach constructs counterfactual outcomes by matching pre-crisis trajectories using weighted combinations of control observations. However, this requires that control units remain unaffected by treatment—violated in financial networks where crisis impacts propagate through exposures.

Alternative specifications of our spatial DID approach yield similar estimates: asset-weighted aggregation produces  $\hat{\tau} = +1,204$  (2.4 % larger), and using heteroskedasticity-robust standard errors instead of bootstrap yields identical point estimate ( $\hat{\tau} = +1,176$ ) with moderately larger standard error (267 versus 218). These specifications validate our baseline approach.

The methodological lesson is that network spillovers require specialized treatment. Standard causal inference methods developed for independent observations systematically overstate treatment effects by attributing spillover impacts to direct treatment. Our spatial DID approach resolves this by aggregating to network level, properly accounting for within-network propagation while maintaining causal interpretation.

## **6 Robustness Analysis**

This section presents extensive robustness checks examining sensitivity to alternative specifications, sample definitions, and measurement approaches.

### **6.1 Alternative Network Specifications**

Table 7 examines sensitivity to network construction choices including exposure thresholds, normalization methods, and weight transformations.

Table 7: Robustness: Alternative Network Specifications

Network Specification	lambda 2 (2007Q2)	Treatment Effect	Std. Error	Change from Baseline
<i>Baseline:</i>				
Geometric mean normalization	1,719	1,176	218	–
<i>Alternative Normalizations:</i>				
Arithmetic mean	1,634	1,089	197	– 7.4 %
Maximum exposure	1,891	1,243	229	+ 5.7 %
Asset-weighted	1,782	1,221	234	+ 3.8 %
<i>Alternative Thresholds:</i>				
Top 10 % exposures only	1,456	987	189	– 16.1 %
Top 25 % exposures only	1,598	1,101	203	– 6.4 %
All exposures (no threshold)	1,719	1,176	218	–
<i>Alternative Weights:</i>				
Binary (unweighted)	1,287	843	174	– 28.3 %
Log-transformed	1,615	1,098	206	– 6.6 %
Square-root transformed	1,683	1,134	212	– 3.6 %

*Notes:* This table examines sensitivity of results to network construction choices. Each row uses alternative specification to construct adjacency matrix and compute algebraic connectivity. lambda 2 (2007Q2) is pre-crisis baseline algebraic connectivity. Treatment Effect is coefficient on Post-2008 indicator from equation (36). Standard Error from bootstrap (1,000 replications). Change from Baseline computes %age difference in treatment effect relative to geometric mean normalization. All specifications include controls from Table 3 Column (4).

Results are qualitatively robust across alternative specifications. Using arithmetic mean normalization instead of geometric mean produces treatment effect  $\hat{\beta} = +1,089$  (7.4 % smaller). Using maximum exposure normalization yields  $\hat{\beta} = +1,243$  (5.7 % larger). Asset-weighted networks produce  $\hat{\beta} = +1,221$  (3.8 % larger). All estimates remain large, positive, and highly statistically significant.

Focusing only on top exposures reduces algebraic connectivity and treatment effects as expected: excluding smaller bilateral relationships lowers network density and coupling. Using top 10 % exposures yields  $\hat{\beta} = +987$  (16.1 % smaller), while top 25 % yields  $\hat{\beta} = +1,101$  (6.4 % smaller). These specifications may be more appropriate if small exposures do not transmit meaningful contagion, though our baseline includes all exposures to fully capture network structure.

Alternative weight transformations produce similar results. Unweighted (binary) networks yield  $\hat{\beta} = +843$  (28.3 % smaller), as binary coding discards information about exposure intensity. Log-transformation yields  $\hat{\beta} = +1,098$  (6.6 % smaller), attenuating influence of largest exposures. Square-root transformation yields  $\hat{\beta} = +1,134$  (3.6 % smaller), intermediate between unweighted and baseline.

## 6.2 Pre-Trends Tests and Placebo Analysis

Table 8 formally tests the parallel trends assumption using leads of the crisis indicator.

Table 8: Pre-Trends Test: Leads of 2008 Crisis Indicator

Lead Period	Coefficient	Std. Error	95 % CI	P-value
2007Q1 (6 quarters before)	- 67	143	[- 353, + 219]	0.639
2007Q3 (4 quarters before)	- 89	156	[- 401, + 223]	0.571
2008Q1 (2 quarters before)	+ 42	134	[- 226, + 310]	0.754
2008Q3 (Crisis quarter)	+ 2,834	476	[+ 1,882, + 3,786]	< 0.001
Joint F-test (all leads)			F = 0.54	0.658

*Notes:* This table tests parallel trends assumption by regressing algebraic connectivity on leads of Post-2008 indicator plus controls. Each row shows coefficient on indicator for specified quarter. Leads (6, 4, 2 quarters before crisis) should be zero under parallel trends. Crisis quarter (2008Q3) shows sharp increase as expected. Standard errors from bootstrap (1,000 replications). Joint F-test examines whether all lead coefficients are jointly zero. Failure to reject ( $p = 0.658$ ) supports parallel trends assumption.



All pre-crisis lead coefficients are small and statistically indistinguishable from zero. The lead 6 coefficient is  $\hat{\beta}_{-6} = -67$  (s.e. = 143, p = 0.639), lead 4 is  $\hat{\beta}_{-4} = -89$  (s.e. = 156, p = 0.571), and lead 2 is  $\hat{\beta}_{-2} = +42$  (s.e. = 134, p = 0.754). The joint F-test fails to reject that all leads are zero (F = 0.54, p = 0.658), strongly supporting the parallel trends assumption.

In contrast, the crisis quarter coefficient is  $\hat{\beta}_0 = +2,834$  (s.e. = 476, p < 0.001), demonstrating sharp discontinuous increase in fragility coinciding with Lehman bankruptcy. This pattern—flat pre-trends followed by sharp increase—is the signature of a valid quasi-experiment.

Table 9 presents placebo tests using alternative crisis dates.

Table 9: Placebo Tests: Alternative Crisis Dates

Placebo Date	Treatment Effect	Std. Error	95 % CI	Expected Result
2006Q3 (2 years early)	- 87	168	[- 423, + 249]	Zero
2007Q3 (1 year early)	+ 134	187	[- 240, + 508]	Zero
2008Q3 (Actual crisis)	+ 2,834	476	[+ 1,882, + 3,786]	Positive
2009Q3 (1 year late)	+ 176	203	[- 230, + 582]	Zero
2010Q3 (2 years late)	- 92	194	[- 480, + 296]	Zero

*Notes:* This table reports placebo tests using artificial crisis dates. Each row estimates equation (36) with Post indicator defined relative to specified placebo date. Standard errors from bootstrap (1,000 replications). Expected Result column indicates whether significant effect is expected under correct identification. Only actual crisis date (2008Q3) should produce significant positive coefficient. Placebo dates before and after should produce insignificant coefficients. Results confirm this pattern, validating identification strategy.

Placebo tests confirm that only the actual crisis date produces significant effects. Using crisis dates 2 years early (2006Q3) yields  $\hat{\beta} = -87$  (s.e. = 168, p = 0.605), 1 year early (2007Q3) yields  $\hat{\beta} = +134$  (s.e. = 187, p = 0.474), 1 year late (2009Q3) yields  $\hat{\beta} = +176$  (s.e. = 203, p = 0.387), and 2 years late (2010Q3) yields  $\hat{\beta} = -92$  (s.e. = 194, p = 0.636).

All placebo coefficients are small and statistically insignificant, while the actual crisis date yields  $\hat{\beta} = +2,834$  ( $p < 0.001$ ). This validates that the observed effect represents causal impact of the 2008 crisis rather than spurious correlation or trend breaks.

### 6.3 Subperiod Analysis

Table 10 examines whether treatment effects vary across different post-crisis subperiods.

Table 10: Subperiod Analysis: Crisis Impact Over Time

Period	lambda 2 Mean	Treatment Effect	Std. Error	Relative to Pre-Crisis
Pre-Crisis (2007Q1-2008Q2)	1,719	—	—	—
Acute Crisis (2008Q4-2009Q4)	3,847	+ 2,128	398	+ 124 %
Recovery (2010Q1-2012Q4)	4,523	+ 2,804	412	+ 163 %
European Debt Crisis (2013Q1-2015Q4)	5,187	+ 3,468	456	+ 202 %
Post-Reform (2016Q1-2019Q4)	6,034	+ 4,315	489	+ 251 %
COVID Era (2020Q1-2021Q4)	6,723	+ 5,004	523	+ 291 %
Recent (2022Q1-2023Q4)	6,984	+ 5,265	537	+ 306 %

*Notes:* This table examines treatment effects separately for different post-crisis subperiods. lambda 2 Mean is average algebraic connectivity for specified period. Treatment Effect is coefficient on period indicator relative to pre-crisis baseline from specification with all controls. Standard Error from bootstrap (1,000 replications). Relative to Pre-Crisis computes %age change from pre-crisis mean of 1,719. Treatment effects increase monotonically over time, demonstrating amplification rather than dissipation.

Treatment effects increase monotonically across subperiods, rising from +124 % in the acute crisis phase to +306 % in the recent period (2022-2023). This pattern confirms dynamic amplification documented in the event study: rather than dissipating as markets adjust, the crisis impact intensified over fifteen years through network evolution and consolidation dynamics.

The acceleration during the European debt crisis (2013-2015) reflects increased interconnectedness as banks maintained exposures to troubled sovereigns despite rising risk. The further acceleration during post-reform period (2016-2019) paradoxically coincides with implementation of Basel III capital requirements, suggesting that regulations may have inadvertently increased coupling by forcing banks to concentrate relationships among approved counterparties.

## 6.4 Alternative Sample Definitions

Table 11 examines sensitivity to sample inclusion criteria.

Table 11: Robustness: Alternative Sample Definitions

Sample Definition	Number of Institutions	Treatment Effect	Std. Error	Change from Baseline
Baseline (G-SIBs plus large banks)	156	1,176	218	—
Only G-SIBs	30	1,423	287	+ 21.0 %
All banks (including small)	412	934	176	— 20.6 %
US banks only	23	1,298	312	+ 10.4 %
European banks only	87	1,067	243	— 9.3 %
Balanced panel (no exits)	142	1,154	214	— 1.9 %
Full sample (including exits)	189	1,234	229	+ 4.9 %

*Notes:* This table examines sensitivity to sample inclusion criteria. Baseline includes 156 institutions designated as G-SIBs or with assets exceeding 100 billion USD. Only G-SIBs restricts to 30 Financial Stability Board designated systemically important banks. All banks includes smaller regional institutions. US/European subsamples restrict geography. Balanced panel drops institutions that exited during sample period. Full sample includes all institutions observed in any period. Standard errors from bootstrap. Change from Baseline computes %age difference in treatment effect relative to baseline sample.

Results are qualitatively similar across sample definitions. Restricting to G-SIBs only yields larger treatment effect ( $\hat{\beta} = +1,423$ , 21 % above baseline), consistent with hypothesis

that largest institutions experienced greater interconnectedness increases. Including all banks yields smaller effect ( $\hat{\beta} = +934$ , 20.6 % below baseline), as small banks participate less in international wholesale funding markets. Geographic subsamples produce similar results to baseline: US banks  $\hat{\beta} = +1,298$  (10.4 % above), European banks  $\hat{\beta} = +1,067$  (9.3 % below).

Balanced panel and full sample specifications yield nearly identical estimates to baseline, indicating that survivorship bias is minimal. Banks that exited (through failure or merger) do not drive the main results.

## 7 Policy Implications and Applications

This section discusses policy implications of our findings for macroprudential regulation, capital requirements, resolution planning, and stress testing.

### 7.1 Network-Targeted Capital Requirements

A key application of our framework is designing capital requirements that optimally reduce systemic risk. Standard Basel III capital requirements apply uniform risk weights to different asset classes but do not account for network externalities: a bank's contribution to systemic risk depends on its position in the network, not just its balance sheet.

We propose network-targeted capital requirements that impose higher requirements on institutions with high spectral centrality. Specifically, institution  $i$ 's capital requirement should be:

$$K_i = K_0 + \alpha \cdot v_{2,i}^2 \cdot Assets_i \quad (39)$$

where  $K_0$  is the baseline Basel III requirement (currently 8 % of risk-weighted assets),  $v_{2,i}$  is institution  $i$ 's Fiedler centrality (component  $i$  of eigenvector  $\mathbf{v}_2$ ), and  $\alpha$  is a policy parameter governing the strength of network adjustment.

Table ?? simulates the impact of network-targeted requirements under alternative values of  $\alpha$ .

Table 12: Network-Targeted Capital Requirements: Counterfactual Analysis

Policy Scenario	Avg Req (%)	Std Dev (%)	lambda-2 Level	Reduction (%)	Banks Affected
Baseline (Uniform 8%)	8.0	0.0	7,151	–	156
Network-Targeted ( $\alpha = 0.05$ )	8.4	1.3	6,234	12.8	47
Network-Targeted ( $\alpha = 0.10$ )	9.1	2.1	5,438	24.0	62
Network-Targeted ( $\alpha = 0.15$ )	9.8	2.9	4,782	33.1	73
Network-Targeted ( $\alpha = 0.20$ )	10.6	3.7	4,231	40.8	89
Size-Based (Top 30 banks)	11.2	4.8	5,987	16.3	30
Leverage-Based (Lev > 15)	10.3	3.9	6,123	14.4	52

*Notes:* This table simulates counterfactual capital requirements under alternative targeting schemes. Baseline applies uniform 8 % requirement on all banks. Network-Targeted adds adjustment proportional to squared Fiedler centrality ( $v-2-i$ ), controlled by alpha. lambda-2 Level is algebraic connectivity under counterfactual policy. Reduction is %age decline in lambda-2 relative to baseline. Banks Affected counts institutions facing requirements above baseline. Size-Based targets 30 largest banks (G-SIBs). Leverage-Based targets high-leverage institutions.

Network-targeted requirements with  $\alpha = 0.15$  reduce algebraic connectivity 33.1 % from 7,151 to 4,782 while requiring only 73 institutions (47 % of the sample) to hold capital above the 8 % baseline. This compares favorably to size-based targeting (top 30 banks), which achieves only 16.3 % reduction despite imposing substantial requirements (11.2 % average) and higher compliance costs (389 billion USD versus 356 billion).

The superiority of network targeting stems from exploiting spectral structure. Banks with high Fiedler centrality sit at network bottlenecks where they contribute disproportionately to connectivity. Reducing their bilateral exposures through capital requirements disrupts contagion pathways more effectively than targeting largest banks, which may have large balance sheets but peripheral network positions.

## 7.2 Stress Testing with Network Dynamics

Current stress testing frameworks evaluate individual institutions' ability to withstand adverse scenarios but do not fully incorporate network amplification of shocks. We propose augmenting stress tests with network diffusion analysis using the continuous functional framework.

Consider a stress scenario where institution  $i$  experiences initial shock  $s_i$ . The system response evolves according to the diffusion equation:

$$\frac{d\mathbf{x}}{dt} = -\mathbf{L}\mathbf{x} + \mathbf{s} \quad (40)$$

where  $\mathbf{x}(t) = [x_1(t), \dots, x_n(t)]$  represents institutions' stress levels at time  $t$  and  $\mathbf{s} = [s_1, \dots, s_n]$  is the shock vector. The equilibrium stress distribution is:

$$\mathbf{x}^* = \mathbf{L}^{-1}\mathbf{s} \quad (41)$$

The amplification factor—ratio of total equilibrium stress to initial shock—is:

$$AF = \frac{\sum_i x_i^*}{\sum_i s_i} = \mathbf{1}^T \mathbf{L}^{-1} \mathbf{s} / \mathbf{1}^T \mathbf{s} \quad (42)$$

Table 13 computes amplification factors for different shock scenarios.

Table 13: Stress Testing with Network Amplification

Shock Scenario	Initial Stress	Equilibrium Stress	Amplification Factor	Most Affected Institutions
Single large bank failure	100	1,142	11.4	Connected G-SIBs
Three regional bank failures	75	623	8.3	Regional networks
Sovereign default (European)	200	2,387	11.9	European banks
Market liquidity shock	150	1,698	11.3	Market makers
Average across scenarios	131	1,463	10.7	—

*Notes:* This table computes network amplification factors for different stress scenarios using the network diffusion model in equation (40). Initial Stress is total shock magnitude (arbitrary units). Equilibrium Stress is steady-state total stress after network propagation. Amplification Factor is ratio of equilibrium to initial stress, measuring network magnification. Most Affected Institutions indicates which bank types experience largest stress increases. Scenarios calibrated to plausible magnitudes based on 2008 crisis events.

Network amplification factors range from 8.3 to 11.9 across scenarios, averaging 10.7. This implies that a shock affecting one institution with initial severity 100 generates equilibrium system stress of 1,070 after propagating through bilateral exposures. Current stress tests that ignore network amplification underestimate systemic impacts by approximately one order of magnitude.

The policy implication is that stress testing frameworks should incorporate network diffusion analysis to accurately assess system-wide consequences. Regulators should evaluate not just whether individual banks survive shocks but whether the network as a whole remains stable accounting for cascading failures and exposure amplification.

### 7.3 Resolution Planning and Too-Big-to-Fail

Our consolidation paradox finding has direct implications for resolution planning. The Dodd-Frank Act requires G-SIBs to prepare "living wills" describing how they would be



wound down in bankruptcy without taxpayer support. However, our analysis suggests that traditional resolution planning may be insufficient when network fragility is high.

Consider the impact of resolving (orderly shutting down) institution  $i$  on system fragility. Removing node  $i$  changes the Laplacian from  $\mathbf{L}$  to  $\mathbf{L}_{-i}$  where row  $i$  and column  $i$  are deleted. The change in algebraic connectivity is:

$$\Delta\lambda_2 = \lambda_2(\mathbf{L}_{-i}) - \lambda_2(\mathbf{L}) \approx v_{2,i}^2 \quad (43)$$

where  $v_{2,i}$  is institution  $i$ 's Fiedler centrality. Institutions with large  $v_{2,i}^2$  contribute substantially to network fragility, making their resolution beneficial for systemic stability.

Table ?? ranks institutions by resolution impact.

Table 14: Resolution Priority Ranking by Network Impact

Institution (Anonymous)	Assets (USD T)	Fiedler Centrality (v-2-i)	Resolution Impact (squared)	lambda-2 Reduction	Fragility Reduction (%)	Priority Rank
Bank A	3.2	0.187	0.035	7,151 to 6,901	3.5	1
Bank B	2.8	0.173	0.030	7,151 to 6,937	3.0	2
Bank C	2.4	0.159	0.025	7,151 to 6,972	2.5	3
Bank D	3.6	0.156	0.024	7,151 to 6,980	2.4	4
Bank E	2.1	0.148	0.022	7,151 to 6,994	2.2	5
...	...	...	...	...	...	...
Average (Top 10)	2.9	0.164	0.027	—	2.7	—
Average (All 156)	0.52	0.048	0.002	—	0.2	—

*Notes:* This table ranks institutions by their contribution to network fragility, measured through squared Fiedler centrality. Institution identities anonymized for confidentiality. Total Assets in trillions USD as of 2023Q4. Fiedler Centrality is absolute value of eigenvector component v-2-i. Resolution Impact equals v-2-i squared, measuring change in lambda-2 from removing institution. lambda-2 Reduction shows counterfactual algebraic connectivity after resolution. Fragility Reduction is %age decline in lambda-2. Priority Rank indicates resolution ordering that maximally reduces systemic risk. Top 10 institutions account for 27 % of fragility reduction despite representing 6.4 % of total banks.

The top 10 institutions ranked by Fiedler centrality contribute 27 % of potential fragility reduction through resolution, despite representing only 6.4 % of banks. This concentration indicates that resolution planning should prioritize these systemically important network hubs. Importantly, the ranking differs from simple size ranking: Bank D has largest balance sheet (3.6 trillion USD) but only fourth-highest network impact because its exposures are relatively diversified.

The policy implication is that "too-big-to-fail" should be redefined as "too-connected-to-fail." Resolution priorities should target network centrality rather than asset size. This requires collecting bilateral exposure data to compute spectral centrality measures—currently not systematically done by most regulators.

## 7.4 International Coordination

Our finding of effectively global contagion propagation (spatial boundary 47,474 kilometers) implies that financial stability is a global public good requiring international coordination. Unilateral national regulations may be ineffective when shocks transmit rapidly across borders through bilateral exposures.

Consider two countries, Home and Foreign, that can each impose capital requirements. The payoff to Home from imposing requirement  $k_H$  when Foreign imposes  $k_F$  depends on network structure:

$$\pi_H(k_H, k_F) = -C(k_H) - \gamma \cdot \lambda_2(k_H, k_F) \quad (44)$$

where  $C(k_H)$  is the cost of imposing requirement  $k_H$  and  $\gamma\lambda_2$  represents expected crisis costs proportional to network fragility. The Nash equilibrium  $(k_H^*, k_F^*)$  satisfies first-

order conditions, but will be inefficiently low due to coordination failure: neither country internalizes the benefit of reducing fragility for the other.

Table 15 simulates equilibrium under alternative coordination regimes.

Table 15: International Policy Coordination: Game-Theoretic Analysis

Coordination Regime	Capital Requirement (%)	lambda 2 Level	Expected Crisis Cost (USD Billion)	Efficiency Gain (%)
No Coordination (Nash)	8.4	6,847	342	–
Bilateral Agreement	9.6	5,923	296	13.5
Full Coordination (Social Optimum)	11.2	4,891	245	28.4
Basel III (Actual)	8.0	7,151	358	– 4.7

*Notes:* This table compares outcomes under alternative international coordination regimes using a two-country game-theoretic model. No Coordination is Nash equilibrium where each country optimizes unilaterally. Bilateral Agreement has countries jointly optimize capital requirements. Full Coordination is social optimum maximizing joint welfare. Basel III (Actual) shows current policy. Capital Requirement is equilibrium or optimal requirement. lambda 2 Level is resulting network fragility. Expected Crisis Cost computed as probability times severity times GDP. Efficiency Gain is %age reduction in expected cost relative to no coordination. Model calibrated using estimated parameters.

Full international coordination achieves 28.4 % reduction in expected crisis costs relative to Nash equilibrium through higher capital requirements (11.2 % versus 8.4 %) and lower fragility (lambda 2 = 4,891 versus 6,847). Bilateral agreements achieve intermediate gains (13.5 %). Notably, actual Basel III requirements (8.0 %) produce even higher costs than Nash equilibrium, suggesting that international coordination is currently insufficient.

The policy implication is that financial regulation requires strengthened international institutions. The Basel Committee on Banking Supervision provides a coordination mechanism, but lacks enforcement power. Our analysis suggests that coordinated capital requirements targeting network centrality could reduce expected crisis costs by nearly 30

% relative to uncoordinated policies—a substantial efficiency gain justifying institutional investment in coordination mechanisms.

## 8 Conclusion

This paper develops and empirically implements a unified framework for analyzing systemic risk in financial networks by integrating spatial treatment effect methodology with spectral network fragility analysis. Building on continuous functional methods from Kikuchi (2024c), Kikuchi (2024f), and Kikuchi (2024i), we characterize contagion dynamics through the spectral properties of network Laplacian operators and identify causal impacts using spatial difference-in-differences methods adapted for interconnected systems.

Our empirical analysis of the 2008 financial crisis yields four principal findings. First, the crisis caused a large, statistically significant, and persistent increase in network fragility measured by algebraic connectivity. Fragility rose 68.4 % above pre-crisis baselines (95 % CI: [42.7 %, 94.1 %],  $p < 0.001$ ) and continued amplifying rather than dissipating over fifteen years, demonstrating structural hysteresis where systems settle into new equilibria rather than reverting automatically.

Second, we document a consolidation paradox: while the number of major banks declined 47.3 % between 2007 and 2023, network fragility increased 315.8 %. This occurred because bilateral exposure concentration rose 687 %, with surviving institutions becoming more tightly coupled. The correlation between exposure concentration and fragility is  $r = 0.97$  ( $p < 0.001$ ), confirming that coupling strength drives systemic risk more than institution count. This finding challenges conventional wisdom that consolidation enhances stability and suggests that post-crisis regulatory reforms may have inadvertently increased systemic vulnerability.

Third, spatial decay analysis reveals that financial contagion exhibits negligible geographic attenuation with spatial decay rate  $\kappa = 0.00002$  per kilometer, implying spatial boundary  $d^* = 47,474$  kilometers—effectively global propagation. This contrasts sharply

with technology diffusion documented in Kikuchi (2024j), which exhibits spatial boundary of only 69 kilometers. The 2,150-fold difference in propagation range reflects distinct mechanisms: financial contagion occurs through instantaneous electronic payment systems, while technology diffusion requires localized face-to-face interactions.

Fourth, traditional difference-in-differences methods that treat institutions as independent units produce treatment effect estimates biased upward by 73.2 %. This bias stems from double-counting spillovers: when one institution experiences crisis impact, connected institutions experience indirect impacts through bilateral exposures. Naive estimators incorrectly attribute both effects to direct treatment. Our spatial difference-in-differences approach resolves this by aggregating to network level before differencing, properly accounting for within-network propagation while maintaining causal interpretation.

The theoretical framework provides several insights. Theorem 1 establishes the consolidation paradox: fragility increases when consolidation occurs if average bilateral exposure intensity grows faster than the inverse of node reduction. The condition  $\bar{w}_1/\bar{w}_0 > n_0/n_1$  determines whether fewer institutions generate higher fragility. In our data, this condition holds with substantial margin ( $\bar{w}_1/\bar{w}_0 = 7.87$  versus  $n_0/n_1 = 1.90$ ), explaining the observed increase.

The integration of spatial decay and network contagion through equation (17) yields testable predictions about relative channel importance. For financial networks, we find  $\kappa \approx 0$  and large  $\lambda_2$ , indicating dominant network channel with minimal geographic friction. For technology diffusion, Kikuchi (2024j) finds large  $\kappa$  and moderate  $\lambda_2$ , indicating dominant spatial channel with important network effects. This demonstrates that the continuous functional framework applies broadly across economic contexts but with dramatically different parameter values.

The policy implications are substantial. First, network-targeted capital requirements that impose higher requirements on institutions with high spectral centrality achieve 33.1 % reduction in fragility while affecting only 47 % of institutions. This compares favorably to size-based targeting, which achieves 16.3 % reduction despite higher compliance costs. Second, stress testing frameworks should incorporate network diffusion analysis to accurately assess system-wide impacts, as our estimates suggest network amplification factors average 10.7 across shock scenarios. Third, resolution planning should prioritize network centrality rather than asset size, redefining "too-big-to-fail" as "too-connected-to-fail." Fourth, international coordination on capital requirements could reduce expected crisis costs by 28.4 % relative to uncoordinated policies.

Our analysis has several limitations that suggest directions for future research. First, we do not observe all bilateral exposures directly, requiring maximum entropy imputation for missing links. While this approach produces minimally informative estimates, access to complete supervisory data would strengthen inference. Second, we treat network structure as exogenous to the crisis, while institutions likely adjusted exposures strategically in response to stress. Developing identification strategies that account for endogenous network formation remains an important challenge. Third, we focus on cross-border exposures among major institutions, omitting domestic interbank markets and shadow banking connections that may transmit contagion. Extending the analysis to include these channels would provide more comprehensive systemic risk assessment.

Fourth, our spatial difference-in-differences approach assumes parallel trends at network level, which we validate using pre-crisis data. However, unobserved time-varying factors could violate this assumption. Instrumental variables strategies exploiting plausibly exogenous variation in network structure could provide additional identification. Fifth,

we analyze a single crisis (2008 financial crisis), limiting external validity. Replicating the analysis for other financial crises—such as the 1997 Asian financial crisis or 2011 European debt crisis—would test generalizability of the consolidation paradox and other findings.

Sixth, we do not model heterogeneous institution responses to the crisis. Banks differed in their strategic responses based on business models, regulatory constraints, and management quality. Allowing for treatment effect heterogeneity could reveal important distributional consequences. Seventh, our stress testing analysis uses linear diffusion dynamics, while actual contagion may exhibit nonlinearities such as threshold effects where shocks exceeding critical values trigger cascading failures. Incorporating nonlinear dynamics would improve realism.

Despite these limitations, our analysis demonstrates that continuous functional methods from mathematical physics provide empirically relevant tools for analyzing systemic risk in financial networks. The finding that consolidation paradoxically increased fragility challenges dominant policy narratives and suggests that post-crisis regulatory reforms may have inadvertently undermined the stability they sought to enhance. Network-targeted interventions that exploit spectral structure offer promising alternatives to conventional size-based regulations. More broadly, the framework applies across economic domains—from technology diffusion to financial contagion—providing unified mathematical foundations for understanding spatial treatment effects in interconnected systems.



## References

- Abadie, A., Athey, S., Imbens, G. W., & Wooldridge, J. (2020). Sampling-based versus design-based uncertainty in regression analysis. *Econometrica*, 88(1), 265–296.
- Acemoglu, D., Ozdaglar, A., & Tahbaz-Salehi, A. (2015). Systemic risk and stability in financial networks. *American Economic Review*, 105(2), 564–608.
- Adrian, T., & Shin, H. S. (2010). Liquidity and leverage. *Journal of Financial Intermediation*, 19(3), 418–437.
- Allen, F., & Gale, D. (2000). Financial contagion. *Journal of Political Economy*, 108(1), 1–33.
- Bardoscia, M., Battiston, S., Caccioli, F., & Caldarelli, G. (2015). Pathways towards instability in financial networks. *Nature Communications*, 6, 6627.
- Battiston, S., Puliga, M., Kaushik, R., Tasca, P., & Caldarelli, G. (2012). DebtRank: Too central to fail? Financial networks, the FED and systemic risk. *Scientific Reports*, 2, 541.
- Bernanke, B. S. (2010). Causes of the recent financial and economic crisis. *Statement before the Financial Crisis Inquiry Commission*, September 2.
- Brunnermeier, M. K. (2009). Deciphering the liquidity and credit crunch 2007-2008. *Journal of Economic Perspectives*, 23(1), 77–100.
- Butts, K., Dickstein, M., & Shapiro, J. (2017). Revisiting event study designs. *NBER Working Paper No. 23474*.
- Cao, Y., & Liu, Y. (2021). Estimating dynamic treatment effects in event studies with heterogeneous treatment effects. *Journal of Econometrics*, 225(2), 175–199.

- Chinazzi, M., Davis, J. T., Ajelli, M., Gioannini, C., Litvinova, M., Merler, S., ... & Vespignani, A. (2020). The effect of travel restrictions on the spread of the 2019 novel coronavirus (COVID-19) outbreak. *Science*, 368(6489), 395–400.
- Demirgüç-Kunt, A., Pedraza, A., & Ruiz-Ortega, C. (2020). Banking sector performance during the COVID-19 crisis. *World Bank Policy Research Working Paper*, No. 9363.
- Elliott, M., Golub, B., & Jackson, M. O. (2014). Financial networks and contagion. *American Economic Review*, 104(10), 3115–3153.
- Fiedler, M. (1973). Algebraic connectivity of graphs. *Czechoslovak Mathematical Journal*, 23(2), 298–305.
- Freixas, X., Parigi, B. M., & Rochet, J. C. (2000). Systemic risk, interbank relations, and liquidity provision by the central bank. *Journal of Money, Credit and Banking*, 32(3), 611–638.
- Gai, P., & Kapadia, S. (2010). Contagion in financial networks. *Proceedings of the Royal Society A*, 466(2120), 2401–2423.
- Garratt, R., Mahadeva, L., & Svirydzenka, K. (2014). Mapping systemic risk in the international banking network. *Journal of Money, Credit and Banking*, 46(s1), 231–257.
- Glasserman, P., & Young, H. P. (2015). How likely is contagion in financial networks? *Journal of Banking & Finance*, 50, 383–399.
- Gorton, G., & Metrick, A. (2012). Securitization. In G. M. Constantinides, M. Harris, & R. M. Stulz (Eds.), *Handbook of the Economics of Finance* (Vol. 2, pp. 1–70). Elsevier.

- Hautsch, N., Schaumburg, J., & Schienle, M. (2015). Financial network systemic risk contributions. *Review of Finance*, 19(2), 685–738.
- Kikuchi, T. (2024a). A unified framework for spatial and temporal treatment effect boundaries: Theory and identification. *arXiv preprint arXiv:2510.00754*.
- Kikuchi, T. (2024b). Stochastic boundaries in spatial general equilibrium: A diffusion-based approach to causal inference with spillover effects. *arXiv preprint arXiv:2508.06594*.
- Kikuchi, T. (2024c). Spatial and temporal boundaries in difference-in-differences: A framework from Navier-Stokes equation. *arXiv preprint arXiv:2510.11013*.
- Kikuchi, T. (2024d). Nonparametric identification and estimation of spatial treatment effect boundaries: Evidence from 42 million pollution observations. *arXiv preprint arXiv:2510.12289*.
- Kikuchi, T. (2024e). Nonparametric identification of spatial treatment effect boundaries: Evidence from bank branch consolidation. *arXiv preprint arXiv:2510.13148*.
- Kikuchi, T. (2024f). Dynamic spatial treatment effect boundaries: A continuous functional framework from Navier-Stokes equations. *arXiv preprint arXiv:2510.14409*.
- Kikuchi, T. (2024g). Dynamic spatial treatment effects as continuous functionals: Theory and evidence from healthcare access. *arXiv preprint arXiv:2510.15324*.
- Kikuchi, T. (2024h). Emergent dynamical spatial boundaries in emergency medical services: A Navier-Stokes framework from first principles. *arXiv preprint arXiv:2510.XXXXX*.
- Kikuchi, T. (2024i). Network contagion dynamics in European banking: A Navier-Stokes framework for systemic risk assessment. *arXiv preprint arXiv:2510.19630*.

- Kikuchi, T. (2024j). Dual-Channel Technology Diffusion: Spatial Decay and Network Contagion in Supply Chain Networks. *arXiv preprint arXiv:2510.XXXXX*.
- Manski, C. F. (2013). Identification of treatment response with social interactions. *The Econometrics Journal*, 16(1), S1–S23.
- Sommese, E., Cerchiello, P., & Torri, G. (2021). A spectral analysis of interbank networks. *Expert Systems with Applications*, 168, 114270.
- Upper, C. (2011). Simulation methods to assess the danger of contagion in interbank markets. *Journal of Financial Stability*, 7(3), 111–125.
- Upper, C., & Worms, A. (2004). Estimating bilateral exposures in the German interbank market: Is there a danger of contagion? *European Economic Review*, 48(4), 827–849.

# A Computational Algorithms

## A.1 Eigenvalue Computation

For computing the algebraic connectivity  $\lambda_2$  of large graphs ( $n = 156$  nodes), we use the Lanczos algorithm for sparse symmetric matrices:

---

**Algorithm 1** Compute Algebraic Connectivity  $\lambda_2$

---

```
1: Input: Laplacian matrix  $L$  in  $\mathbb{R}^{n \times n}$ 
2: Output: Algebraic connectivity  $\lambda_2$ 
3: Initialize random vector  $v_0$  in  $\mathbb{R}^n$  orthogonal to  $\mathbf{1}$ 
4: Normalize:  $v_0$  becomes  $v_0$  divided by  $\|v_0\|_2$ 
5: for  $j = 1$  to  $k$  (number of Lanczos iterations) do
6:    $w$  becomes  $L v_{j-1}$ 
7:    $\alpha_j$  becomes  $v_{j-1}^T w$ 
8:    $w$  becomes  $w - \alpha_j v_{j-1}$ 
9:   if  $j > 1$  then
10:     $w$  becomes  $w - \beta_{j-1} v_{j-2}$ 
11:   end if
12:    $\beta_j$  becomes  $\|w\|_2$ 
13:    $v_j$  becomes  $w / \beta_j$ 
14:   Construct tridiagonal matrix  $T_j$  from  $\alpha_i, \beta_i$ 
15:   Compute eigenvalues of  $T_j$  using QR algorithm
16: end for
17: Return: Second smallest eigenvalue of  $T_k$ 
```

---

## A.2 Bootstrap Inference

For constructing confidence intervals robust to clustering and heteroskedasticity:

---

**Algorithm 2** Bootstrap Confidence Intervals

---

- 1: **Input:** Network data  $G_t$  for  $t$  equals 1 to  $T$  quarters
- 2: **Input:** Number of bootstrap replications  $B$  equals 1000
- 3: **Output:** 95 % confidence interval
- 4: Compute point estimate  $\hat{\theta}$  on full sample
- 5: **for**  $b$  equals 1 to  $B$  **do**
- 6:   Sample  $T$  quarters with replacement:  $t_1^*$  through  $t_T^*$
- 7:   Construct bootstrap sample using networks  $G_{t_j^*}$
- 8:   Estimate model on bootstrap sample:  $\hat{\theta}_b$
- 9: **end for**
- 10: Sort bootstrap estimates
- 11: **Return:** 2.5th and 97.5th %iles

---

### A.3 Maximum Entropy Network Imputation

For imputing missing bilateral exposures:

---

**Algorithm 3** Maximum Entropy Imputation

---

- 1: **Input:** Observed exposures  $E_{ij}$  for pairs in  $O$
- 2: **Input:** Row sums  $E_{i-out}$  and column sums  $E_{j-in}$
- 3: **Output:** Complete exposure matrix  $E$
- 4: Initialize  $E_{ij}$  equals  $E_{ij-obs}$  for pairs in  $O$
- 5: **for** iteration equals 1 to max-iterations **do**
- 6:   **for** all unobserved pairs  $i, j$  not in  $O$  **do**
- 7:      $E_{ij}$  becomes  $E_{i-out}$  times  $E_{j-in}$  divided by  $E_{total}$
- 8:   **end for**
- 9:   Rescale rows:  $E_{ij}$  becomes  $E_{ij}$  times  $E_{i-out}$  divided by  $\sum_j E_{ij}$
- 10:   Rescale columns:  $E_{ij}$  becomes  $E_{ij}$  times  $E_{j-in}$  divided by  $\sum_i E_{ij}$
- 11:   Check convergence: if maximum absolute row column deviation less than tolerance, break
- 12: **end for**
- 13: **Return:** Complete matrix  $E$

---